Deep Impact's Target Comet 9P/Tempel 1 at Multiple Apparitions: Seasonal and Secular Variations in Gas and Dust Production

David G. Schleicher

Lowell Observatory
1400 W. Mars Hill Road
Flagstaff, Arizona 86001

To be published in *Icarus*
Original submission: 21 November 2006
Revised and accepted: 13 April 2007

The Lowell Observatory Preprint Series

Deep Impact's Target Comet 9P/Tempel 1 at Multiple Apparitions: Seasonal and Secular Variations in Gas and Dust Production

David G. Schleicher

Lowell Observatory, 1400 W. Mars Hill Road, Flagstaff, Arizona 86001
E-mail: dgs@lowell.edu

ABSTRACT

We present results from multi-apparition narrowband photometry of Deep Impact target Comet 9P/Tempel 1. In support of the mission, we obtained data during monthly observing runs between March and September 2005, and these are combined with and compared to observations obtained during the 1983 and 1994 apparitions. A strong seasonal effect is seen, with peak production rates occurring 4-8 weeks before perihelion, with some variation evident among the different species. There is also evidence of a slight systematic shift towards a later time of peak production in 2005 as compared to 1983. Early in the apparition, the radial profile of the dust was much steeper than the canonical $1/\rho$, but the slope became progressively smaller until very little departure from $1/\rho$ remained by late June, a change possibly associated with the general seasonal effects. Unexpectedly, an unprecedented large overall decrease in production rates has taken place since 1983, with water at only about 42% of the 1983 values, CN at about 53%, and dust, based on the proxy $A(\theta)f\rho$, at about 77%. Other gas species exhibited declines intermediate between that of CN and of the dust. The large differences in the amount of secular decline among all of the species implies compositional inhomogeneities among source regions on the surface of the nucleus, with one region progressively becoming less active over only a few orbits. While the simplest explanation would invoke either devolatilization or covering up of the ice, no other comet has shown such a rapid change in outgassing unless accompanied by a significant change in its orbit. We, therefore, hypothesize that a change in available solar radiation due to precession of the pole might instead be causing the progressive drop in cometary activity. Given the small obliquity of the rotation axis derived from the Deep Impact observations, and a presumed small rate of precession, the source region would need to be located near the pole to explain both the large secular and seasonal trends.

Key Words: Tempel 1, comets, coma, composition, photometry

1. INTRODUCTION

To study the physical structure and interior composition of cometary bodies, the nucleus of Comet 9P/Tempel 1 was successfully hit by NASA's Deep Impact spacecraft on 4 July 2005 (A'Hearn et al. 2005). In support of this unique event, expected to excavate a crater and blast new material into the coma, telescopes from both around the world and in space provided near-continuous coverage of Tempel 1 in the days surrounding the collision (cf. Meech et al. 2005, Keller et al. 2005; Lisse et al. 2006; Feldman et al. 2007). Many of the same observers, including ourselves, also obtained a variety of measurements of the comet over much longer time intervals to characterize what constituted typical or baseline behavior so that any short or long-term modifications to the nucleus and/or coma caused by the impact could be identified, and to provide ongoing water and dust measurements to the DI team and to predict conditions at the time of the encounter.

Comet Tempel 1 was also of considerable interest to us because we had previously determined that peak gas production rates occurred about 7 weeks prior to perihelion in 1983 rather than when the comet was closest to the Sun (Osip et al. 1992), thereby implying that the comet experienced significant seasonal variations. In spite of the comet's faintness post-perihelion due to observing circumstances coupled with the seasonal fall-off, to support the Deep Impact mission we made a significant effort to extend the temporal coverage beyond what our group had obtained in 1983. Finally, because the orbit of Tempel 1 has been largely unperturbed for more than 30 years, it made a good subject to search for long-term secular trends in the rate of nucleus outgassing.

The results from our intensive 12-day observing campaign of photometry and imaging surrounding the Deep Impact encounter have previously been reported (Schleicher et al. 2006a), including determination of baseline production rates, measurements of post-impact brightening and subsequent return to baseline values, and successful modeling of the ejecta plume. A detailed study of the rotationally varying gas and dust coma morphology of Tempel 1 is in progress and will be presented elsewhere. Here we present the results from our monthly photometry observing campaign from March to September 2005, along with photometric measurements made during the comet's 1994 apparition and rereduced measurements from 1983. We also discuss our findings regarding Tempel 1's seasonal and secular behavior and place these into the context of the results discerned by the Deep Impact team.

2. OBSERVATIONS AND REDUCTIONS

2.1 Instrumentation

All observations of Comet 9P/Tempel 1 presented here were obtained with conventional photoelectric photometers and narrowband comet filters. During the 1983 apparition, all data except for those from one night were taken using the Perkins 72-inch (1.8-m) telescope at Lowell Observatory; the additional night was taken with the 24-inch (0.6-m) Planetary Patrol telescope at Perth Observatory. For the 1994 and 2005 apparitions, all successful measurements were either obtained with the John S. Hall 42-inch (1.2-m) or the 31-inch (0.8-m) telescopes at Lowell Observatory; two additional nights were attempted from Perth but these data proved unusable. The detectors were a pair of EMI 6256 photomultiplier tubes (one at each

observatory). Filters from three different epochs were employed: In 1983 the original A'Hearn and Millis (AM) set was used at Lowell, while a newly acquired International Halley Watch (IHW) set was used at Perth; in 1994 an old but still good quality IHW set was used, along with a degrading NH filter from the AM set, for which a linearly interpolated correction factor for the flux of 1.62 was automatically applied; and Hale-Bopp (HB) sets were used in 2005. Note that while the same emission bands are isolated by successive generations of filter sets, the location of the continuum passbands has changed. Specifically, the green continuum was originally centered at 5240 Å, then 4845 Å for the IHW set, and is now at 5260 Å. The UV continuum has gone from 3675 Å to 3650 Å to 3448 Å, and a new intermediate continuum filter at 4450 Å was introduced with the HB set. Therefore, the color of the dust needs to be accounted for when making comparisons of the continuum obtained with different filter sets.

2.2 Observations

Between one and four photometric sets were successfully obtained on each of 37 nights, resulting in a total of 88 sets over the three apparitions. Each set typically consisted of 5 gas filters, isolating emission from OH, NH, CN, C_3, and C_2, along with 2-3 continuum filters, but occasionally fewer filters were used due to a lack of time or to the faintness of the comet. The comet was usually observed in each filter for several 10-30 second integrations, and these were either followed by or interspersed with separate sky measurements more than 15 arcmin away from the comet. Observational circumstances for each night are summarized in Table 1, including the heliocentric and geocentric distances as well as the phase angle of Tempel 1. The diameter of the photometer entrance aperture ranged between 14 and 155 arcsecs, while the corresponding projected aperture radius (ρ) varied between 3,900 and 43,700 km. The mid-time and the aperture size for each observational set are listed in Table 2. Comet flux standard stars were measured to determine nightly extinction coefficients and instrumental corrections for each filter.

2.3 Reductions

The 2005 data were reduced to fluxes using the procedures and coefficients detailed by Farnham et al. (2000) for the HB filter set, while the data obtained during the previous apparitions were rereduced using the revised procedures and coefficients for the AM and IHW sets given in the appendix of Farnham and Schleicher (2005) based on the HB methodology of Farnham et al. (2000). In particular, as compared to the original reductions, this resulted in improved decontamination of the ultraviolet and green continuum filters of the wings of the C_3 and C_2 emission bands, respectively, and improved extinction corrections for the OH observations in the near-UV.

The resulting fluxes for each gas species, listed in Table 2, were then converted to column abundances and production rates (see Table 3) using our standard procedures given by A'Hearn et al. (1995). In the cases of OH, NH, and CN, the required fluorescence efficiencies (L/N) vary with heliocentric velocity ($\dot{r}_H$) and, in the case of CN, distance, and the nightly values are given in Table 1. As usual, the Haser model (Haser 1957) is simply used to extrapolate to a total coma abundance from the column abundance, and then production rates are derived by dividing by the assumed daughter scalelengths (again tabulated in A'Hearn et al.). For OH, which has only the one parent, H_2O, and reasonably well constrained parent and daughter lifetimes and velocities, we also derive the water production rate using the empirical relation derived by

Cochran and Schleicher (1992) and discussed by Schleicher et al. (1998). In the case of continuum filters, we derive the quantity $A(\theta)f\rho$ as defined by A'Hearn et al. (1984) — the product of the dust albedo at the given phase angle, the filling factor for the aperture, and the projected aperture radius. This proxy for dust production requires no assumptions regarding the particle size distribution, and yields a value independent of aperture size and wavelength if the dust grains are gray in color and have a canonical $1/\rho$ radial distribution.

In addition to the uncertainties associated with photon statistics for each comet measurement, on a few nights possible systematic errors were relatively large due to poor determination of extinction coefficients. In such cases, we have estimated the contribution and included this effect into the tabulated 1-sigma uncertainties given in Table 3 and displayed in each of the figures.

3. PHOTOMETRIC RESULTS

3.1 Production Rates vs Distance, Time, and Apparition: An Overview

We first present gas production rates and $A(\theta)f\rho$ for the green continuum as a function of heliocentric distance (r_H) in a series of log-log plots in Figure 1. Each apparition is distinguished by a different symbol, and it is immediately evident that all species exhibited significantly larger production rates in 1983 than in 2005 as we initially reported during the 2005 apparition (Schleicher and Barnes 2005); we will discuss this characteristic in detail below. It is also readily apparent that, except for the brightening associated with the Deep Impact ejection plume, gas production rates reach a peak at a distance of about 1.6 AU, nearly 2 months before perihelion. The dust, as characterized by $A(\theta)f\rho$, reaches a peak even earlier, but as we will later show, this difference from the gas is due to phase angle effects. As expected, given this early production peak, production rates following perihelion (filled symbols) are systematically lower than those at comparable heliocentric distances before perihelion, although it is unclear if this asymmetry would continue at larger distances than those for which we have observations.

Because the pre-perihelion production rates cannot be reasonably represented by a linear fit (in these log-log plots), and the post-perihelion baseline is relatively short, we have chosen not to attempt to determine r_H-dependencies for Tempel 1. However, we do note that all of the gas species exhibit considerably steeper trends with r_H before peak production than does the dust, and this difference remains even after adjusting the dust measurements for phase angle effects.

To more easily examine the asymmetric behavior of the production rates, in Figure 2 we plot the data as a function of time from perihelion, using the same symbols as in Figure 1. An expanded version of the cluster of points surrounding perihelion and the Deep Impact encounter has previously been presented (using nightly averages) by Schleicher et al. (2006a). The overall asymmetry with respect to perihelion is obvious during both 1983 and 2005; the 1994 observational interval was too limited to determine a time of peak production, but the downward trend between the two 1994 observing runs is completely consistent with the behavior evident in 1983 and in 2005 for this same interval. Therefore, to first order, the bulk temporal or seasonal trend appears to be the same for each of the apparitions, and is very similar for each of the gas species.

In contrast to the similar nature of the seasonal trends for each species, the amount of secular decrease from the 1983 apparition to the 2005 apparition appears to differ considerably among the various species: The OH production rate drops by a factor of 2.5, NH and CN drop by about a factor of 1.9, while C_2 and C_3 apparently only decrease by between factors of 1.4 and 1.5. The dust, as characterized by $A(\theta)f\rho$, has a large amount of apparent scatter in the first half of the 2005 apparition, and shows a drop from 1983 by between factors of about 1.5 and 2.4, depending on the time from perihelion.

We emphasize, however, that all but one night's observations obtained during 1983 were made with smaller photometer entrance apertures than available in the later apparitions, due to the differing plate scales of the telescopes used. As a consequence, one must check if the secular decrease is real or simply an artifact associated with the differing aperture sizes and/or the particular viewing geometries, and the values given above will be revisited in Section 3.4 after examining these issues in detail. Fortunately, with a orbital period of almost exactly 5.5 years, every other apparition (i.e. those at which the comet is favorably placed) has a nearly identical viewing geometry; the dates and perihelion distances for the observed apparitions were 1983 July 9.8 (q=1.491 AU), 1994 July 3.3 (1.494 AU), and 2005 July 5.3 (1.506 AU). We can, therefore, eliminate viewing geometry as the cause of the observed secular decrease (or of any other measured variation between these three apparitions). We can also eliminate changes in species' lifetime associated with the solar cycle, since the length of the solar cycle is commensurate with the observed apparitions, and the solar cycle was near minimum activity each apparition. It is evident, therefore, that any trends with aperture size which might exist should be expected to repeat for all three apparitions.

3.2 Aperture Size Effects and Adjustments

As evident from Tables 2 and 3, the 1983 observations with the Perkins 72-inch telescope used aperture diameters ranging from 14 to 40 arcsec, and a range of projected radii from 3900 to 12000 km. All other observations were taken with aperture diameters of between 36 and 156 arcsec, and projected radii of between 10000 and 43700 km. Fortunately, the large range of aperture sizes employed on many individual nights in 2005 allow us to directly check for possible trends with aperture size in the derived production rates. One indication can be discerned from the amount of scatter visible in Figure 2. In the cases of OH, NH, and CN, data points are tightly grouped when the uncertainties are small, even when the aperture size varied by factors of 3 or more — directly implying that the Haser scalelengths used in our reduction to production rates closely reproduce the observed radial distribution of these species. Plots of production rates as a function of the log of the projected radii of representative nights during the 2005 apparition are given in Figure 3. Specifically, monthly sets of 1-2 nights of data from early March to early July are presented; there was an insufficient range of aperture sizes measured later in the apparition due to the faintness of the comet. These plots confirm that only quite small trends with radius are present for OH and CN. For instance, the OH decreases slightly with increasing aperture radius, for a log-log slope of -0.08. This results in a slightly smaller amount of secular decrease from 1983 to 2005 than presented in Section 3.1 — a factor of 2.4 rather than 2.5. In fact, OH is the only gas species showing a negative slope with aperture size. CN, exhibiting a neutral or slightly increasing production rate with aperture size for an average slope of +0.06, has a very slightly larger secular drop than originally computed, as does NH, with an average aperture slope of only about +0.03. C_2 and C_3, which exhibited larger scatter within individual observing runs than did the other

gas species, both have larger positive trends in production rate vs aperture size, with average log-log slopes of +0.10. The aperture corrected results for the secular decreases will be discussed in detail in Section 3.4.

The largest apparent dispersion among data sets in Figure 2 was exhibited by the dust as characterized by $A(\theta)f\rho$, and this dispersion is due to a strong trend with aperture size, as shown both in Figure 3 and the top panel of Figure 4. Somewhat unexpectedly, the aperture trend for the dust varies greatly during the apparition, with the steepest departure from a canonical $1/\rho$ radial distribution for the dust (which would have yielded the same $A(\theta)f\rho$ value at every aperture size) occurring at the beginning of the apparition, with this departure from $1/\rho$ decreasing until it was nearly gone by perihelion and the Deep Impact encounter. It is unclear what would cause such a large change in the dust's radial distribution over only 4 months of time, but it may be associated with the strong seasonal effect exhibited by Tempel 1. Whatever the cause of this change, we can use the slopes derived in the fits of log $A(\theta)f\rho$ vs log ρ at different dates (see Figure 3) to derive a quadratic fit of the aperture slopes as a function of time from perihelion. Using this relation, we can then normalize all observations to a common projected aperture radius, 1×10^4 km, with the results shown in the bottom panel of Figure 4. Generally, to within the individual uncertainties, the large dispersion seen among the 2005 data in the top panel is removed, more clearly revealing the underlying secular variations. (As described next in Section 3.3, an adjustment for phase angle has also been applied to the data shown in the bottom panel of Figure 4.)

3.3 Dust Phase Angle Effects

As noted earlier in Section 3.1, the dust appears to have a peak in $A(\theta)f\rho$ about a month earlier than the peak seen in all of the gas species' production rates. This shift in location is simply due to phase angle effects, with a minimum phase angle of 11.°1 occurring during the 2005 apparition on April 2, 93 days prior to perihelion. By the time of perihelion, only a day after the Deep Impact encounter, the phase angle increases to 41.0°, and reaches a maximum of 41.°6 in late July. The variation of the phase angle with time from perihelion for 2005 is shown as the dashed curve in the middle panel of Figure 4. (Due to the nearly identical viewing circumstances, the phase curves for 1983 and 1994 differ only slightly from the 2005 curve shown.)

To compensate for the enhanced back scattering at small phase angles, we have adjusted all of the dust observations using the phase function derived by Schleicher et al. (1998) from measurements of Comet 1P/Halley. As shown by Schleicher et al., photometry of Halley's dust at small (<20°) phase angles exhibited a significantly steeper phase dependence than what has sometimes been assumed, such as the function of Devine (1981). Schleicher et al. derived a quadratic fit to the Halley data: log $A(\theta)f\rho = -0.01807 \times \theta + 0.000177 \times \theta^2$, where theta is the phase angle in degrees. Note that this function works well for phase angles smaller than about 45-50°, but at larger phase angles it rises too quickly and deviates from the phase dependencies observed in a variety of comets, and so should not be used at phase angles greater than about 50°. When applying the Halley phase function (or any other phase function) to adjust for phase effects, we have a choice as to what phase angle we normalize to. Because of the large number of data sets obtained near the time of the Deep Impact encounter, we have chosen an angle of 41°, the phase angle at perihelion. The Halley phase function adjustment of log $A(\theta)f\rho$ to log $A(41°)f\rho$ is shown as the solid curve in the middle panel of Figure 4.

The effect of this phase correction is presented in the bottom panel of Figure 4, where the normalization for aperture size from Section 3.2 has also been applied. The phase corrected peak in $Af\rho$ is now shifted to between about -60 and -30 days from perihelion and within the range of times measured for the various gas species.

3.4 Long-term Secular Decrease

By intercomparing the resulting ensemble of aperture and phase adjusted $Af\rho$ values for 2005 with those from 1983, one discovers that the 2005 values are on average only a factor of 1.3 lower than in 1983, a much smaller decrease than one would originally infer from Figure 2. The apparent variation in the amount of secular decrease as a function of time from perihelion (i.e. season) has also been mostly but not entirely eliminated.

Based on the aperture trends determined in Section 3.2, we can similarly make the much smaller adjustments of each gas species' measurements to a common aperture, and can reinvestigate the secular variations by simply shifting an entire apparition's log production rates up or down to best match the envelope of production rates for each of the other apparitions. From 1983 to 2005, the production rates of C_2 and C_3 decrease by factors of 1.6 and 1.5, respectively. CN and NH have secular decreases by factors of 1.9 and 2.1, respectively, while OH continues to exhibit the largest decrease, a factor of 2.4. We estimate the uncertainties on the relative values between 1983 and 2005 to be about 3-5%. Therefore, while the larger aperture trends exhibited by C_2 and C_3 partially explain the smaller secular decreases seen for these species in Figure 2, significant differences remain in the amount of secular decrease among the gas species. Variations are also observed among the species as to the degree of decrease seen during the 1994 apparition, but these values are much more uncertain (about 10-15%) because few observational sets were obtained, and specific values are therefore subject to either rotational effects, sporadic outbursts (see Section 3.6), or seasonal variations among the various species. Our best estimates for the overall secular offsets for the three apparitions are summarized in Table 4, while the effects of adjusting each species' values by these amounts to yield overall seasonal variations is displayed in Figure 5 and discussed in Section 3.5.

Evidence for a possible secular decrease has previously been reported. The first such claim was made by Haken et al. (1995) based on *IUE* measurements of OH in 1983 and 1994, where an apparent decrease by a factor of ~2.5 took place based on a single 1994 observation. However, issues regarding pointing and tracking of the comet, high scattered light in the instrument near the end of *IUE*'s lifetime, and possible but unknown rotational variability, made the specific amount of the secular decrease in OH highly uncertain (see also Lisse et al. 2005). The claimed OH decrease was also suspect simply because other species did not exhibit comparable decreases from 1983 to 1994, either in the Lowell datasets or those from the McDonald Observatory spectrophotometry survey (Cochran et al. 1992; Lisse et al. 2005). In retrospect, it is evident that the limited number of 1994 measurements are intermediate to the 1983 and 2005 results, and that OH (and therefore water) production has dropped by a greater amount than has the production of the other, minor gas species and the dust.

These differences in the amount of the secular decrease among the various gas species and the even greater difference between the water and the dust raises a possibly serious problem: Since it is the gas production

which measures the vaporization of the ice, and the dust is released and lifted by the resulting gas flow, why should the dust decrease by only 23% when the water production has dropped by 58%? As previously noted, this cannot be an artifact due to viewing geometry or lifetimes associated with solar activity because of the near-identical circumstances at each apparition.

We conclude that the only reasonable explanation is that there are compositional inhomogeneities between two or more source regions on the surface of the nucleus. Furthermore, one source is dramatically decreasing its rate of water vaporization since 1983 but that this source has lower abundances of minor gas species and of dust, resulting in a smaller secular decrease in the bulk coma abundances for these species. The simplest explanation for the rapid decrease in vaporization rates for a source region would be the devolatilization or covering up of the ice, as has often been invoked to explain why dynamically older comets have much smaller fractions of their surface still active as compared to dynamically young comets (cf. Whipple 1978; A'Hearn et al. 1995). However, it is perhaps unlikely that significant crusting over or devolatilization could occur on such a short timescale as 2 decades, especially as many other short-period comets have shown no significant secular changes (cf. A'Hearn et al. 1995).

This brings us to a third possible mechanism: A source region receiving significantly less sunlight from one apparition to the next due to a significant change in the orientation of the rotation pole, such as might be caused by simple precession. Comet 2P/Encke provides one example, where Sekanina (1991) has claimed Encke's pole has precessed by about 40° during just over a century. More recently, fitting the observed polar jet in Comet 19P/Borrelly both in the early 1900's and in the 1994 and 2001 apparitions revealed a total precession of about 8° since the 1911-1932 time frame (Schleicher et al. 2003). While we know of no evidence of rapid precession in the case of Tempel 1, such as large changes in the non-gravitational parameters describing its orbit (cf. Yeomans et al. 2005; Davidsson et al. 2007), a relatively small precession might be sufficient to cause a large secular change in unique circumstances. As this issue is closely associated with the Deep Impact spacecraft dataset, we will return to this issue in Section 4.

3.5 Seasonal Variations

Based on the measured secular changes given in Table 4 for each species, we can effectively adjust the measurements obtained during 1983 and 1994 to those for 2005, eliminating the secular effects and permitting us to examine the seasonal variations shown in Figure 2 in more detail. The resulting apparitional lightcurves are shown in Figure 5, excluding data associated with the Deep Impact ejecta. For clarity of overlapping points, all data are now plotted as open symbols, with different symbols again distinguishing the three apparitions.

Except for the dust, which exhibits shallower curvature overall, all species show the same general shape, with peak production taking place between about 55 and 25 days before perihelion. However, some detailed differences are now visible: for instance, based on the shapes of each curve, C_2, C_3, and NH each appear to have peak production about 4-5 weeks before perihelion while the peaks for OH, CN, and dust occur about 6-8 weeks before perihelion. Furthermore, the data for each species exhibit a small shift in the time of peak production with respect to perihelion, with peaks apparently taking place about 5-10 days earlier in 1983 than during 2005. However, some of these variations may be an artifact of a somewhat undersampled

apparitional lightcurve coupled with rotational effects (see next sub-section). The net result is that we have suggestive but not conclusive evidence for small changes in the seasonal trends during an interval of only a few apparitions, but that the gross seasonal characteristics repeat from 1983 to 2005.

We can check and extend the shape of our seasonal lightcurve for dust in 2005 with the results from the CARA (Cometary Archive for Amateur Astronomers) campaign, where most observations were obtained using broadband R CCD imaging (Milani et al. 2007). The consortium of CARA observers were able to obtain both a more extensive and denser temporal coverage than we could acquire. Their $A(\theta)f\rho$ results, uncorrected for phase angle, show a peak in dust production near -80 days, while correcting to constant phase angle with an assumed phase function gives a peak near -50 days (their Figures 4 and 5); each are in excellent agreement with our own results. The CARA results also show a steep rise in $A(\theta)f\rho$ beginning 6-7 months prior to perihelion, followed by a more shallow decline. These results can further be compared to reduced magnitude measurements of Tempel 1 from the 1994 apparition compiled by Ferrín (2005; 2007). His temporal magnitude plots show an initial turn-on for the comet (i.e. brightness greater than nuclear) about 7 months before perihelion, followed by a steep rise and then a shallower decay post-perihelion, not returning to nuclear brightness until more than a year after perihelion. This reaffirms our conclusion that the overall seasonal lightcurve repeats over several apparitions, and this shape needs to be accounted for in any comprehensive model of nucleus activity.

Large seasonal effects, with either strong pre-/post-perihelion asymmetries in production rates and/or significant offsets for the time of peak production with respect to perihelion, have been observed in many comets (cf. A'Hearn et al. 1995). And in each of the few cases for which we have determined nucleus rotational pole orientations based on coma morphology, the rotation axis has had a high obliquity, resulting in a large variation in the sub-solar latitude as the comet orbited the Sun consistent with production rate asymmetries. In one such case, Comet 19P/Borrelly, we were even able to quantitatively reproduce the water production rates as a function of time using the same nucleus model with a polar source region as was derived from the coma jet morphology throughout the apparition (Schleicher et al. 2003). However, the pole orientation of Comet Tempel 1 as derived by the Deep Impact team from imaging of the nucleus has only an 11° obliquity, and from early March to late September (the span of our observations) the sub-solar latitude only varies from -3° to +11°. It therefore seems unlikely that such a small variation in the incident solar radiation could cause such a large seasonal effect as we and others observed unless a fairly special set of circumstances exists. We will also return to this issue in Section 4.

3.6 Rotational Variability

There have been several reports of sporadic or quasi-periodic outbursts of activity for Comet Tempel 1 in the days and weeks preceding the Deep Impact encounter, both detected from the Deep Impact spacecraft (A'Hearn et al. 2005; Farnham et al. 2007) and from the ground (cf. Meech et al. 2005). At least some of these outbursts occurred at the same rotational phase, directly implying their association with a source region on the nucleus, even though the events do not recur every rotational cycle. One must therefore be aware that any individual night's data might be associated with outburst activity. It is, however, clear that the overall seasonal lightcurves discussed previously are dominated by the routine level of activity of the comet, and probably no more then a few individual days of data are affected by outbursts.

Because of the relatively short observing window each night as compared to the rotation period of 41 hr reported from the Deep Impact spacecraft observations during its approach to the comet (A'Hearn et al. 2005), obtaining an unambiguous rotation period from groundbased observations is difficult. Moreover, our only data set suitable for examining rotational variability is the 12-night run surrounding the time of the spacecraft encounter, and the several nights following the encounter are "contaminated" by the material associated with the ejecta plume (Schleicher et al. 2006a). Therefore, instead of attempting to derive the rotation period of the nucleus based on coma variability, we have simply used the published spacecraft result of 1.701±0.014 day (A'Hearn et al. 2005) and phased our observations accordingly, excluding the post-impact point on July 4, and excluding the following 4 nights of observations. As shown by Schleicher et al. (2006a), Tempel 1 had essentially returned to baseline levels for all species by at least July 10 and probably by the 9th.

The resulting phase plots for each species from the 8 nights of included photometry are presented in Figure 6. Zero phase has been set to the time of the impact (July 4, 5^h52^m) as seen from Earth. Production rates for each species have been adjusted for trends with aperture size as described in Section 3.2; this adjustment, at most a 10% effect or 0.04 in the log, generally serves to slightly reduce the scatter among data points taken within an individual night, but does not effect the shape of the phased lightcurves. Dust production, represented by the green continuum $Af\rho$, has also been adjusted for phase angle (see Section 3.3). Finally, we have also removed the secular decline of approximately 1% per day observed for all species for this time frame (Schleicher et al. 2006a) which is associated with the overall seasonal variation described in Section 3.5.

Overall, no strong, large-amplitude rotational variability is evident from these data. However, examining individual species in more detail reveals some rotational signatures in the phased lightcurves. For instance, CN appears to exhibit an asymmetric, double-peaked lightcurve, with an amplitude of about 30%, i.e., a value much greater than the measurement uncertainties. OH appears to exhibit a similarly shaped lightcurve as CN, albeit with quite large uncertainties. Specifically, the phases of the two minima and the first maximum appear to match; however, the second maximum in OH is much less certain. Dust also exhibits characteristics of the CN and OH lightcurves, but the shape is not conclusive. (The inner-most dust coma, ρ <100 km, measured by Deep Impact shows a lightcurve dominated by a single, southern-hemisphere jet turning on and off with rotation; Farnham et al. 2007.) In contrast, NH perhaps exhibits a broad single-peaked lightcurve, with no evident correlation with either the CN nor OH lightcurves, but the reality of this result is difficult to assess due to the large photometric uncertainties. Finally, C_2 and C_3 each show some variability but with no clearly discernable patterns. We note that some differences among species is to be expected — differing lifetimes of the various parent species will yield varying phase lags and, due to dilution from existing coma material, larger aperture sizes will show longer delays and smaller amplitudes than the actual production rate variations on the surface of the nucleus. We further note that since we are measuring coma abundances presumably originating from localized active regions on the nucleus, the double-peaked lightcurve apparently evident in CN and possibly in OH implies the existence of two significant source regions on the surface of the nucleus. This must be distinguished from the asteroidal double-peaked lightcurve measured by Deep Impact which is caused by the changing cross-section of the nucleus.

Biver et al. (2005) initially reported a periodicity of 1.7 day in HCN line intensities, and Biver et al. (2007) show that the HCN data from May 4-9 yield a single-peak lightcurve having an amplitude of about a factor of 3. Unfortunately, the precision of the rotation period is not yet sufficient to unambiguously compare the phasing of our CN data with that of HCN data obtained three months earlier and determine which, if either, of the 2 maxima we identify corresponds to the HCN maximum.

The only other published rotational lightcurves for gas species of which we are aware are those by Jehin et al. (2006) for CN and NH, and the subsequent analyses of the same spectroscopic observations by Manfroid et al. (2007) for CN, NH, NH_2, OH, OI, CH, C_2, and C_3. Their spectroscopic measurements were obtained on 10 nights surrounding the impact (July 2-11) along with 3 nights in early June. When our CN data are phased with the same period (1.709 day) and zero point (time of impact) as used by Jehin et al., we get a lightcurve which has some similar characteristics with Jehin et al.'s, but with a phase shift of about 0.2. Since our aperture is larger than theirs, we would expect some shift, but not this large. We believe the cause of this discrepancy is due to the inclusion of three night's of early June data in the Jehin et al. lightcurve. These points (the 4 highest points near phase 0.1 and two of the highest points near phase 0.7 in Jehin et al.'s Figure 1; personal communication from Jehin) define both the amplitude and phase of the two primary peaks, but we know that the production rates were systematically higher (by 25-30%) in early June as compared to early July. If these 6 data points are excluded (or shifted to lower values to compensate for the long-term trend), the time of maximum light would increase by about 0.05 to 0.10 phase, in better agreement with own results, and with a remaining phase shift of 4-6 hr consistent with expected aperture size effects. Rotational phase plots for other gas species shown by Manfroid et al. have varying amplitudes and scatter, but generally exhibit a stronger feature near phase 0.1-0.2, and a weaker feature near a phase of 0.7, consistent with their CN plot.

Overall, we conclude that the CN shows evidence of a double-peaked lightcurve, with the two peaks about 0.6 phase apart, suggesting that there are at least two significant source regions on the surface, with longitudes about 210-220° apart. [We also suggest that the specific rotation period derived by Jehin et al. be reevaluated after adjusting the early June observations to compensate for the seasonal decline in production rates; the difference in their derived period and that found from the Deep Impact measurements (A'Hearn et al. 2005) might, in part, be an artifact of the seasonal month-to-month decline in activity of the comet.]

3.7 Composition

Given the different amounts of secular decrease seen among the observed species between 1983 and 2005, the relative abundances and the associated composition also must differ at least somewhat over this time interval. We also obtained many more observations in 2005 than in either 1983 or 1994, so an overall average would be strongly weighted towards the 2005 results. For these reasons, we compute abundance ratios (i.e. the production rate ratios) separately for each apparition, and these are listed in Table 5. Here we have used the production rates after adjustment for aperture size trends from Section 3.2, but among the gas species the unadjusted ratios differ relatively little from the adjusted values, and always by less than 15%.

As evident from Table 5, the associated uncertainties are somewhat larger in 2005 than in the previous apparitions. This appears to be due to a combination of factors, but primarily from having numerous lower S/N data points near and following perihelion when production rates were lower caused by general seasonal trend, and from the overall lower S/N in 2005 caused by the secular decrease in the comet's brightness. Additionally, any seasonal variation between species would be magnified in 2005 because of the longer temporal coverage, further contributing to larger uncertainties associated with 2005 averaged results.

Because of the relatively large formal uncertainties on many of the abundance ratios, it is difficult to claim that a definitive change in abundance ratios among the gas species has taken place from 1983 to 2005. In particular, the C_2-to-CN ratio, used in the A'Hearn et al. (1995) taxonomic classification, remains cleanly in the "typical" class at each apparition. But the dust-to-gas ratio, based on the proxies $A(\theta)f\rho$ and Q(OH), does appear to have significantly increased since 1983, as one would expect given that the dust and OH represent the two extremes in the amount of secular decrease. This increase in the dust-to-gas ratio took Tempel 1 from being slightly gassier than average to near-average as compared to other comets in the Lowell database, but the change is relatively small when one considers the 2-order-of-magnitude range in the dust-to-gas ratio among all comets (A'Hearn et al. 1995).

Very similar production rate ratios have been reported by Lara et al. (2006) based on 5 nights of spectrophotometry obtained between 2005 mid-April and mid-June. However, their absolute production rates are consistently more than a factor of 3 below the envelope of our own results; we have no explanation for this large discrepancy since few of our own observations appear to be associated with the occasional outbursts of activity (see discussion in Section 3.6), and both groups state that they use the same g-factors and scalelengths listed in A'Hearn et al. (1995).

3.8 Water

Using the procedure noted in Section 2, we can compute water production rates based on on our OH measurements. Sustained peak production reached 6-7×10^{27} molecule s^{-1} in early May 2005, while by the time of the Deep Impact encounter the typical water production rate had dropped to about 5×10^{27} molecule s^{-1}. For concurrent times of observation and to within the quoted uncertainties for each data set, our results are generally in excellent agreement with those reported by Bensch et al. (2006) based on water measurements with the Submillimeter Wave Astronomy Satellite (SWAS), and by Crovisier et al. (2005) based on radio OH measurements. In the few cases when disagreements are evident, one data point has usually been significantly higher than baseline values, implying that the "odd" point might be the result of an outburst.

The strong seasonal variation seen at both the 1983 and 2005 apparitions implies a significant change in solar illumination of one or more source regions during each apparition. Without knowing the location of the source regions, it is difficult to determine which thermal model is most appropriate for computing the required active area necessary to produce the observed water production. Therefore, until the locations and relative strengths of each source region are clarified, we have chosen to simply use the same vaporization model as used by A'Hearn et al. (1995), which assumed a negligible thermal inertia for a uniformly active nucleus. The resulting first-order size of the effective active area is about 2 km^2 in 2005 and 5 km^2 in 1983,

or between about 5% and 13% of the total nucleus surface based on the spacecraft derived nucleus size with a mean radius of 3.0±0.1 km (A'Hearn et al. 2005).

3.9 Dust Colors

After excluding observations obtained in the days directly following the Deep Impact collision and thus contaminated with ejecta, only small trends in the color of the dust — green vs UV continuum — were observed for several variables, including heliocentric distance, time, and apparition. In fact, all observed trends appear to simply be associated with and a result of a small, underlying trend of the dust color with aperture size. After allowing for the differing continuum filter locations among the three filter sets, the average reddening between the green and UV spectral regions for the smallest apertures is about 29% per 1000Å, while the large apertures exhibit a reddening of about 20% per 1000Å. The unweighted average of all points is 23% per 1000Å, but the formal uncertainty is quite large, 28% per 1000Å, due to the large number of low S/N points in the ultraviolet. Overall, these amounts of reddening would be considered quite moderate and are typical of comets in this spectral regime (e.g. Jewitt and Meech 1986). Finally, with the blue continuum filter introduced with the HB filter set, we can compute a color between the green and blue continuum filters. Here too a similar trend with aperture is seen for the longer baseline into the UV; the resulting reddening between the blue and green filters is about 8% per 1000Å.

4. Summary of Results, Interrelation with Deep Impact, and Discussion

In support of the Deep Impact spacecraft mission, we obtained numerous imaging and photometric observations of Tempel 1 in the days surrounding the encounter (Schleicher et al. 2006a), along with monthly narrowband photoelectric photometry during 2005 beginning in early March and concluding in late September. Our primary goals for the monthly observations were to provide ongoing water and dust measurements to the DI team and to predict conditions at the time of the encounter. These observations were also intended to enable the Deep Impact mission results to be placed into a much broader context than possible solely from a brief flyby mission, by characterizing Tempel 1's seasonal and secular behavior. Furthermore, because the results described in Section 3 were obtained using the same techniques as those determined and discussed by A'Hearn et al. (1995) based on the Lowell comet database, Deep Impact results can potentially be extended to a much larger group of comets known to have properties similar to Tempel 1. We also wanted to extend the temporal arc beyond what our group had obtained during Tempel 1's 1983 apparition, in spite of the difficulty due to the comet's faintness after perihelion, fully expecting to both confirm the seasonal behavior observed at that time and to confirm that, like all of the other comets we've observed at multiple apparitions, little or no inherent secular change had taken place. Obtaining these confirmations was important since critical details of the DI mission plan, such as a safe encounter distance for the flyby spacecraft, were based on constraints largely determined from water and dust measurements obtained during the 1983 apparition (Lisse et al. 2005).

We were successful in our endeavors, although not always in our predictions. A strong seasonal effect was, indeed, again seen in 2005, with peak production rates occurring 4-8 weeks before perihelion, and the specific time of peak varying among the species: maximum production for OH and CN taking place first, followed by C_3, C_2, and finally NH. Peak dust production, based on the proxy $A(41°)f\rho$, occurred at about 6-

7 weeks before perihelion, but this value is less certain because there was a significant but evolving trend of $A(41°)f\rho$ with aperture size prior to perihelion, and thus the date of the peak depends somewhat on which aperture size is examined.

These differences among the species of the time at which peak production took place are most likely the result of a heterogeneity in composition between source regions, with the relative activity of the sources varying differently with season due to being located at differing latitudes on the nucleus. A changing relative proportion of outgassing from multiple sites as Tempel 1 orbits the Sun and the sub-solar latitude varied with time might also provide an explanation for the change in the spatial radial profiles of the dust as a function of time from much steeper than $1/\rho$ early in the apparition to ~$1/\rho$ at and following perihelion. This change in bulk properties of the dust coma could be due to differences in the dust released from source regions, such as particle size or outflow velocity. We will return to this topic later in this section.

Unlike our successful prediction regarding seasonal effects, we were quite surprised by the low production rates exhibited by Tempel 1 in 2005, although in retrospect, evidence for a change from 1983 values was present in our limited 1994 dataset. We are unaware of any other comet which has so rapidly changed its rate of outgassing over only a few apparitions except when there was a significant perturbation of its orbit, as in the cases of 19P/Borrelly (Schleicher et al. 2003) and 81P/Wild 2 (Farnham and Schleicher 2005), or a breakup of the nucleus, as in the case of 73P/Schwassmann-Wachmann 3 (Schleicher et al. 2006b). By 2005, water production in Tempel 1 decreased to only about 42% of its 1983 values, CN to about 53%, and dust, based on the proxy $A(\theta)f\rho$, to about 77%. Other gas species exhibited declines intermediate between that of CN and of the dust. While less certain due to the limited number of observations, production rates in 1994 were generally in between the 1983 and 2005 values. The time at which peak production of each species takes place also appears to have experienced a secular change, with a systematic shift by ~5-10 days later in 2005 as compared to 1983, with this effect presumably associated with or a symptom of the large drop in overall gas and dust production.

By combining these various pieces of evidence, we conclude that there must be 2 or more source regions with appreciable differences in composition, and at least one source region has progressively become much less active during only a few orbits. The simplest explanation for this unprecedented decline in production rates is that a source region experienced significant devolatilization or that the ice had been covered or crusted over by an insulating layer of material, perhaps associated with some of the layering evident in Deep Impact imaging (Thomas et al. 2007), although the fact that no other comet has been observed to change this rapidly implies that these processes usually take place at a much slower rate. Therefore, while we do not rule out either of the standard mechanisms, we suggest that a third, alternative mechanism might instead be at work on Tempel 1. Again, we propose that one source region's level of activity has drastically decreased, but the cause could be a reduction in available solar radiation due to the precession of the rotation axis of the nucleus. Given the small obliquity (11°) of the rotation axis derived from the Deep Impact observations (A'Hearn et al. 2005), and a presumed small rate of precession (Yeomans et al. 2005), the source region would need to be located near a pole.

We noted in Section 3.5 the apparent difficulty in explaining Tempel 1's large seasonal variations in light of the small obliquity of the rotation axis, and claimed a special set of circumstances might be needed to

explain the seasonal behavior. A source region located very near a pole with the sub-solar latitude varying from -3° to +11° during our observing interval can provide just such special case. An otherwise large/strong active source region could receive sufficient sunlight even at a highly oblique sun angle to be active early in the apparition, but mostly shutdown by perihelion (sub-solar latitude of +9°). This scenario is made more attractive since the preliminary shape model of the nucleus has a large, relatively flat region at the south pole (Thomas et al. 2007), implying that enough surface area might be available to yield significant gas vaporization even with a very low angle for the incident sunlight. Our coma jet modeling (work in progress) of groundbased images also implies the existence of a south polar source, along with a second source at the mid-southern latitudes. Deep Impact approach imaging suggests that, in addition to the strong "southern jet" whose northern-most extent is at about -45° and which dominates coma variability, there is also a radial feature ("Jet 4") visible in the inner-most coma which apparently arises from near the south pole (Farnham et al. 2007). Thus there are independent lines of evidence suggesting a south-polar source region.

We tentatively conclude, therefore, that Comet 9P/Tempel 1 has at least 2 source regions, with one located at or very close to the south pole. Only a near-polar source can explain the large seasonal variations seen with a very low-obliquity nucleus. The very need of explaining a strong seasonal effect for an object with a small pole obliquity and thus a small total range in the sub-solar latitude, also provides a viable mechanism for the large secular decrease in production rates since 1983: A precession of only 5° or 10° could greatly reduce the amount of solar radiation which the south-polar source received during the 2005 apparition. The large secular decrease also implies that polar source was likely the primary active source, producing the majority of the total coma when it was in sunlight. Given the low sun angle, this source must also be relatively large in size, consistent with broad expanse in the preliminary shape model of the nucleus. As the south-polar source loses sunlight and decreases its rate of gas production, the dust outflow velocity might also decrease, yielding a possible means of changing the dust bulk radial profiles over time. In any case, the proportion of dust arising from the south-polar region and the other source regions would certainly change, and so differing properties of the dust grains among the source regions, such as the particle size distribution, could also affect the radial profiles. Besides the dust properties, significant chemical inhomogeneities must exist between the south polar source and the other active source region(s), as evidenced by different secular decreases among the observed species and by differences in the rotational lightcurves.

Overall, it is clear that Comet 9P/Tempel 1 has provided an extremely interesting laboratory for studying physical and chemical properties of cometary comae and nuclei, while the synergy between the Deep Impact data and observations from the ground will continue to yield many new insights for years to come.

ACKNOWLEDGEMENTS

We gratefully acknowledge R. Millis for the acquisition of many of the observations, along with P. Birch for his observations from Perth Observatory. We also acknowledge the assistance of N. Baugh and K. Barnes during the Deep Impact time frame. The initial reductions and analyses of the 1983 data set were performed by D. Osip, while A. Bair assisted with reductions of some of the 2005 data. We particularly thank T. Farnham and M. A'Hearn for making Deep Impact spacecraft results available prior to publication and numerous discussions which have assisted our understanding of Comet Tempel 1's behavior. This work was funded by the NASA Planetary Astronomy Program under grant NAG5-13379 and its predecessors.

REFERENCES

A'Hearn, M. F., et al., 2005. Deep Impact: Excavating Comet Tempel 1. Science 310, 258-264.

A'Hearn, M. F., Millis, R. L., Schleicher, D. G., Osip, D. J., and Birch, P. V., 1995. The Ensemble Properties of Comets: Results from Narrowband Photometry of 85 Comets, 1976-1992. Icarus 118, 223-270.

A'Hearn, M. F., Schleicher, D. G., Feldman, P. D., Millis, R. L., Thompson, D. T., 1984. Comet Bowell 1980b. Astron. J. 89, 579-591.

Bensch, F., Melnick, G. J., Neufeld, D. A., Harwit, M., Snell, R. L., Patten, B. M., and Tolls, V., 2006. Submillimeter Wave Astronomy Satellite observations of Comet 9P/Tempel 1 and Deep Impact. Icarus 184, 602-610.

Biver, N., Bockelée-Morvan, D., Colom, P., Crovisier, J., Lecacheux, A., Paubert, G., 2005. Comet 9P/Tempel. IAU Circular 8538.

Biver, N., Bockelée-Morvan, D., Boissier, J., Crovisier, J., Colom, P., Lecacheux, A., Moreno, R., Paubert, G., Lis, D. C., Sumner, M., Frisk, U., Hjalmarson, A., Olberg, M., Winnberg, A., Florén, H.-G., Sandqvist, A., Kwok, S., 2007. Radio observations of Comet 9P/Tempel 1 before and after Deep Impact. Icarus 187, 253-271.

Cochran, A. L., Barker, E. S., Ramseyer, T. F., and Storrs, A. D., 1992. The McDonald Observatory faint comet survey: Gas production in 17 comets. Icarus 98, 151-162.

Cochran, A. L., and Schleicher, D. G., 1993. Observational Constraints on the Lifetime of Cometary H_2O. Icarus 105, 235-253.

Crovisier, J., Colom, P., Biver, N., Bockelée-Morvan, D., and Lecacheux, A., 2005. Comet 9P/Tempel. IAU Circular 8512.

Davidsson, B. J. R., Gutiérrez, P. J., and Rickman, H., 2007. Nucleus properties of Comet 9P/Tempel 1 estimated from non-gravitational force modeling. Icarus 187, 306-320.

Farnham, T. L., and Schleicher, D. G., 2005. Physical and Compositional Studies of Comet 81P/Wild 2 at Multiple Apparitions. Icarus 173, 533-558.

Farnham, T. L., Schleicher, D. G., and A'Hearn, M. F., 2000. The HB Narrowband Comet Filters: Standard Stars and Calibrations. Icarus 147, 180-204.

Farnham, T. L., Wellnitz, D. D., Hampton, D. L., Li, J.-Y., Sunshine, J. M., Groussin, O., McFadden, L. A., Crockett, C. J., A'Hearn, M. F., Belton, M. J. S., Schultz, P., and Lisse, C. M., 2007. Dust Coma Morphology in the Deep Impact Images of Comet 9P/Tempel 1. Icarus 187, 26-40.

Feldman, P. D., McCandliss, S. R., Route, M., Weaver, H. A., A'Hearn, M. F., Belton, M. J. S., and Meech, K. J., 2007. Hubble Space Telescope observations of Comet 9P/Tempel 1 during the Deep Impact encounter. Icarus 187, 113-122.

Ferrín, I., 2005. Secular light curve of Comet 9P/Tempel 1. Icarus 187, 326-331.

Ferrín, I., 2007. Secular light curve of Comet 28P/Neujmin 1 and of spacecraft target Comets 1P/Halley, 9P/Tempel 1,

Haken, M., A'Hearn, M. F., and Feldman, P. D., 1995. Apparent Fading of Comet P/Tempel 1. B.A.A.S. 27, 1472-1473.

Haser, L., 1957. Distribution d'intensite dans la tête d'une comète. Bull. Acad. R. Belgique, Classes des Sci. 43, 740-750.

Jehin, E., Manfroid, J., Hutsemékers, D., Cochran, A. L., Arpigny, C., Jackson, W. M., Rauer, H., Schulz, R., Zucconi, J.-M. 2006. Deep Impact: High-Resolution Optical Spectroscopy with the ESO VLT and the Keck I Telescope. ApJ 641, L145-L148.

Jewitt, D., and Meech, K. J., 1986. Cometary grain scattering versus wavelength, or 'What color is comet dust'? ApJ 310, 937-952.

Keller, H. U., Jorda, L., Küppers, M., Gutiérrez, P. J., Hviid, S. F., Knollenberg, J., Lara, L.-M., Sierks, H., Barbieri, C., Lamy, P., Rickman, H., Rodrigo, R., 2005. Deep Impact Observations by OSIRIS Onboard the Rosetta Spacecraft. Science 310, 281-283.

Lara, L. M., Boehnhardt, H., Gredel, R., Gutiérrez, P. J., Ortiz, J. L., Rodrigo, R., and Vidal-Nuñez, M. J., 2006. Pre-impact monitoring of Comet 9P/Tempel 1, the Deep Impact target. A&A 445, 1151-1157.

Lisse, C. M., A'Hearn, M. F., Farnham, T. L., Groussin, O., Meech, K. J., Fink, U., and Schleicher, D. G., 2005. The Coma of Comet 9P/Tempel 1. Space Science Reviews 117, 161-192.

Lisse, C. M., VanCleve, J., Adams, A. C., A'Hearn, M. F., Fernandez, Y. R., Farnham, T. L., Armus, L., Grillmair, C. J., Ingalls, J., Belton, M. J. S., Groussin, O., McFadden, L. A., Meech, K. J., Schultz, P. H., Clark, B. C., Feaga, L. M., Sunshine, J. M., 2006. Spitzer Spectral Observations of the Deep Impact Ejecta. Science 313, 635-640.

Manfroid, J., Hutsemékers, D., Jehin, E., Cochran, A. L., Arpigny, C., Jackson, W. M., Meech, K., Schulz, R., Zucconi, J.-M. 2007. The impact and rotational light curves of Comet 9P/Tempel 1. Icarus 187, 144-155.

Meech, K. J., et al., 2005. Deep Impact: Observations from a Worldwide Earth-based Campaign. Science 310, 265-269.

Milani, G. A., Szabó, Gy. M., Sostero, G., Trabatti, R., Ligustri, R., Nicolini, M., Facchini, M., Tirelli, D., Carosati, D., Vinante, C., and Higgins, D., 2007. Photometry of comet 9P/Tempel 1 during the 2004/2005 approach and the Deep Impact module impact. Icarus 187, 276-284.

Osip, D. J., Schleicher, D. G., and Millis, R. L., 1992. Comets: Groundbased Observations of Spacecraft Mission Candidates. Icarus 98, 115-124.

Schleicher, D. G., 2006. Compositional and Physical Results for Rosetta's New Target Comet 67P/Churyumov-Gerasimenko from Narrowband Photometry and Imaging. Icarus 181, 442-457.

Schleicher, D., and Barnes, K., 2005. Secular Decrease in Production Rates of Comet 9P/Tempel 1. IAU Circular 8546.

Schleicher, D. G., Barnes, K. L., and Baugh, N. F., 2006a. Photometry and Imaging Results for Comet 9P/Tempel 1 and Deep Impact: Gas Production Rates, Post-Impact Lightcurves, and Ejecta Plume Morphology. Astron. J. 131, 1130-1137.

Schleicher, D. G., Birch, P. V., and Bair, A. N., 2006b. The Composition of the Interior of Comet 73P/Schwassmann-Wachmann 3: Results from Narrowband Photometry of Multiple Fragments. B.A.A.S. 38, 485.

Schleicher, D. G., and Farnham, T. L, 2004. Photometry and Imaging of the Coma with Narrowband Filters. In *Comets II* (M. C. Festou, H. U. Keller, and H. A. Weaver, eds.) Univ. of Arizona, Tucson. 449-469.

Schleicher, D. G., Millis, R. L., and Birch, P. V., 1998. Narrowband Photometry of Comet P/Halley: Variation with Heliocentric Distance, Season, and Solar Phase Angle. Icarus 132, 397-417.

Schleicher, D. G., Woodney, L. M., and Millis, R. L. 2003. Comet 19P/Borrelly at Multiple Apparitions: Seasonal Variations in Gas Production and Dust Morphology. Icarus 162, 415-442.

Thomas, P. C., Veverka, J., Belton, M. J. S., Hidy, A., A'Hearn, M. F., Farnham, T. L., Groussin, O., Li, J.-Y., McFadden, L. A., Sunshine, J., Wellnitz, D., Lisse, C., Schultz, P., Meech, K. J., and Delamere, W. A., 2007. The shape, topography, and geology of Tempel 1 from Deep Impact observations. Icarus 187, 4-15.

Yeomans, D. K., Giorgini, J. D., and Chesley, S. R., 2005. The History and Dynamics of Comet 9P/Tempel 1. Space Science Reviews 117, 123-135.

FIGURE CAPTIONS

Figure 1: Log of the production rates for each observed molecular species and $A(\theta)f\rho$ for the green continuum plotted as a function of the log of the heliocentric distance. Data points from the 1983 apparition are shown as triangles while those from 1994 are given as squares and the recent 2005 data are shown as circles; open symbols represent data obtained before perihelion while filled symbols are used for post-perihelion measurements. Vertical dotted lines represent perihelion distances, with perihelia successively moving slightly further from the Sun. Note the large asymmetries around perihelion for all species, and large secular variations between apparitions.

Figure 2: Same as Figure 1, but production rates are plotted as a function of time from perihelion. Here it is evident that the peak production rates for all gas species were reached 1-2 months before perihelion. The proxy for dust production, $A(\theta)f\rho$, apparently peaked even earlier, but as will be shown, this difference is an artifact of the changing phase angle of the dust. Significant secular decreases from one apparition to the next are also evident for each species. The increase in production rates due to the ejecta released by Deep Impact (ΔT = -1.07 day) are also evident.

Figure 3: Relative log production rate values as a function of the log of the projected aperture radii in 2005. Representative observations from each month are shown with alternating open and shaded symbols when a sufficient range of aperture sizes were used: March 10, April 5&6, May 6&8, June 9, and July 3&4 (prior to impact). Linear fits to each set are shown; each set is normalized to the value of the fit at 1×10^4 km, but shifted vertically based on the time from perihelion (right-hand axis labels). Each of the 5 gas species show relatively small trends with aperture size, except when points of larger photometric uncertainties are involved; implying that the Haser model scalelengths used in the reductions provide a relatively good match to the actual radial distributions of each gas species. Even so, because nearly all of the data from the 1983 apparition were obtained with smaller apertures (3900-12000 km), average aperture corrections based on the observed trends were determined for each gas species (see Table 4 and text for details). Unlike the gas species, the dust exhibits much larger trends with aperture size but which also systematically decreases as the apparition progressed. Thus a functional form of the aperture trend as a function of time was derived for the dust.

Figure 4: Dust $Af\rho$ as a function of time. The top panel shows an expanded version of the green continuum panel from Figure 2, but with different sized symbols representing the various photometer aperture sizes used in the observations. For clarity of overlapping data, open symbols are used for all data points. The middle panel shows the change in phase angle during the 2005 apparition (dashed curve and right-side axis); the curves for 1983 and 1994 are nearly identical. Using the phase function derived by Schleicher et al. (1998) from 1P/Halley observations, an adjustment of $A(\theta)f\rho$ to constant phase angle is shown as the solid curve. This adjustment for phase angle is normalized to the value at perihelion: 41° (see text for details). The bottom panel shows the results, after adjusting for aperture size (Section 3.2) and for phase angle. In this

view it is evident that the secular decrease from 1983 to 2005 is much smaller than seen in Figure 2, but still significant. Also, the time of peak dust production, as based on the proxy $A(41°)f\rho$, is later than it first appeared but still well before perihelion.

Figure 5: Adjusted production rates as a function of time from perihelion. Data are the same as Figure 2, but have been adjusted for aperture size (see Section 3.2) and, in the case of dust, phase angle (Section 3.3). The 1983 and 1994 data have also been normalized to the 2005 observations by the long-term secular decreases given in Table 4 (Section 3.4). Finally, data obtained on the 4 nights following the Deep Impact collision, and thereby containing ejecta contributions, are not included here. For clarity, open symbols are used for all data points. The resulting composite plots better show the seasonal effects for each species. In 2005, the time of peak production varied between 7 and 4 weeks before perihelion, depending on species. In comparison, there is evidence that the time of peak production rates in 1983 were systematically about 5-10 days earlier than in 2005.

Figure 6: Production rates plotted as a function of rotational phase. Phasing is based on the derived period of 1.701 day from the Deep Impact spacecraft observations (A'Hearn et al. 2005) and with zero phase set to the time of impact as seen from Earth — July 4, 5^h52^m UT. Observations from 2005 June 29 to July 4 (prior to impact) are included, along with those from 2005 July 9 and 10, following Tempel 1's return to pre-impact production rate trends. Production rates have been slightly adjusted for aperture size and seasonal trends and, in the case of dust, for phase angle effects (see text for details). CN and perhaps OH show evidence of a double-peaked lightcurve, implying the existence of two source regions on the nucleus' surface. Other species show evidence of short-term variability, but it is less clear if periodic rotational signatures are present.

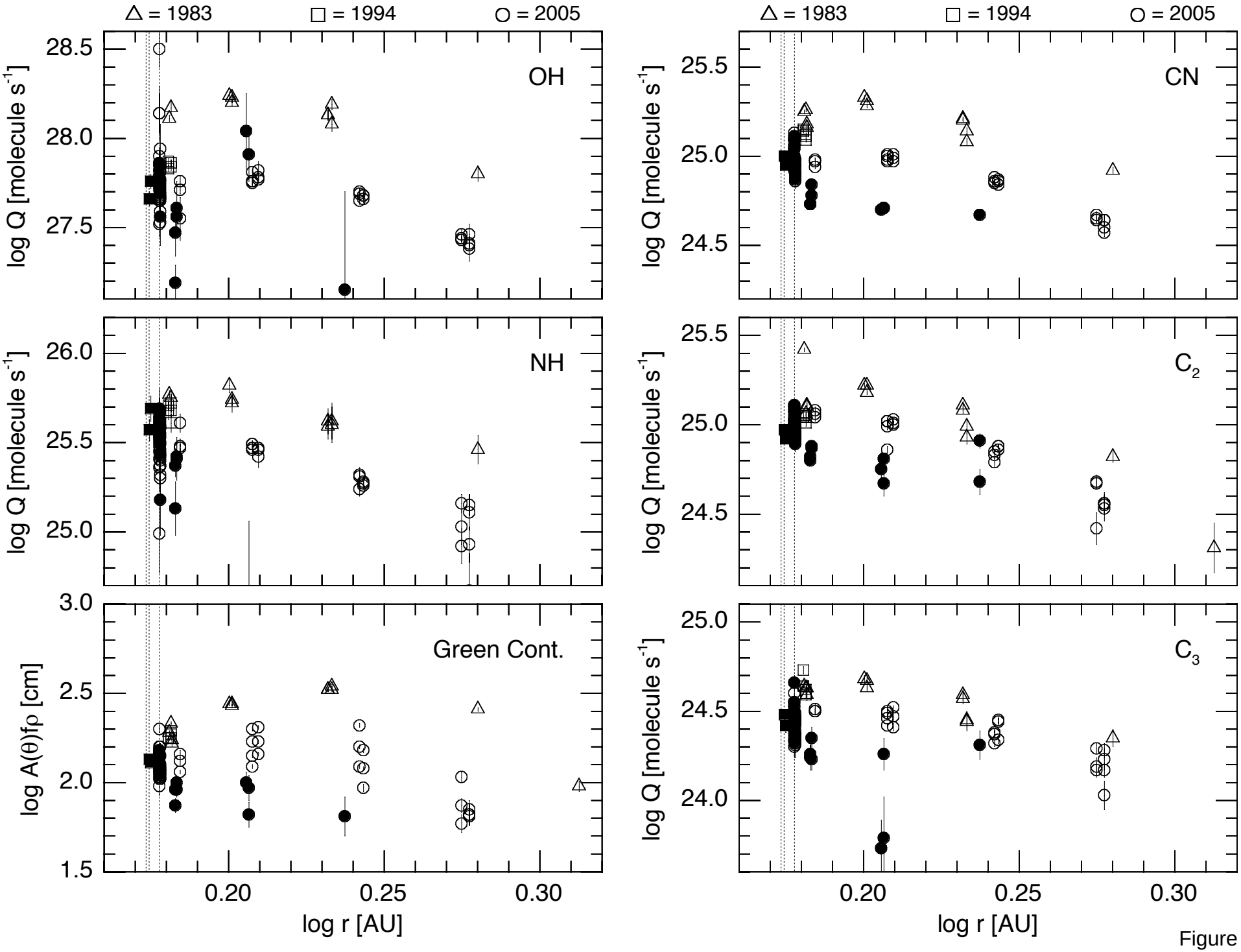
△ = 1983
□ = 1994
○ = 2005
OH
log Q [molecule s^{-1}]
28.5
28.0
27.5
NH
26.0
25.5
25.0
Green Cont.
log A(θ)fρ [cm]
3.0
2.5
2.0
1.5
CN
25.5
25.0
24.5
C$_2$
C$_3$
24.0
0.20
0.25
0.30
log r [AU]

Figure 1

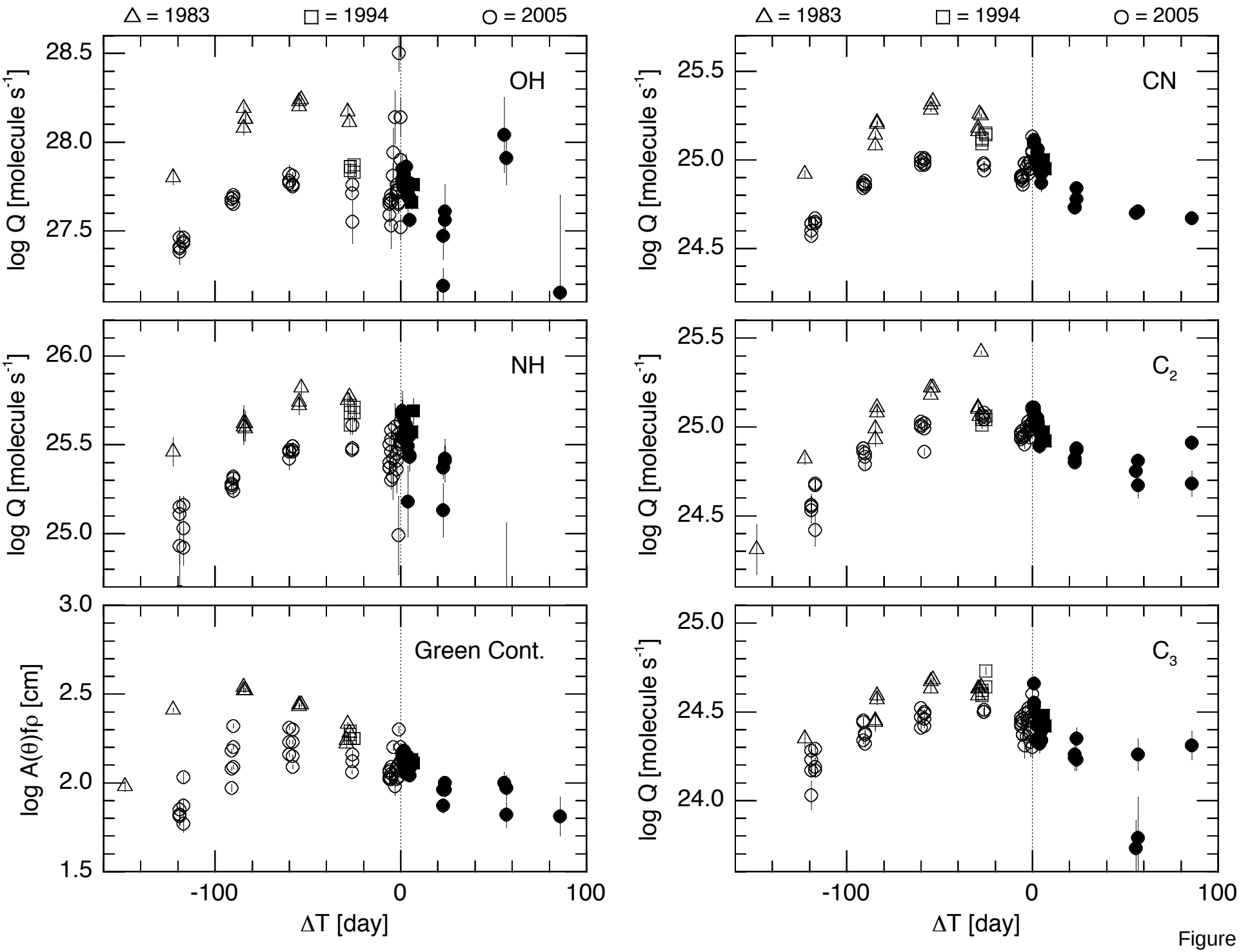
△ = 1983
□ = 1994
○ = 2005
OH
NH
Green Cont.
CN
C2
C3
log Q [molecule s-1]
log A(θ)fρ [cm]
ΔT [day]
-100
0
100

Figure 2

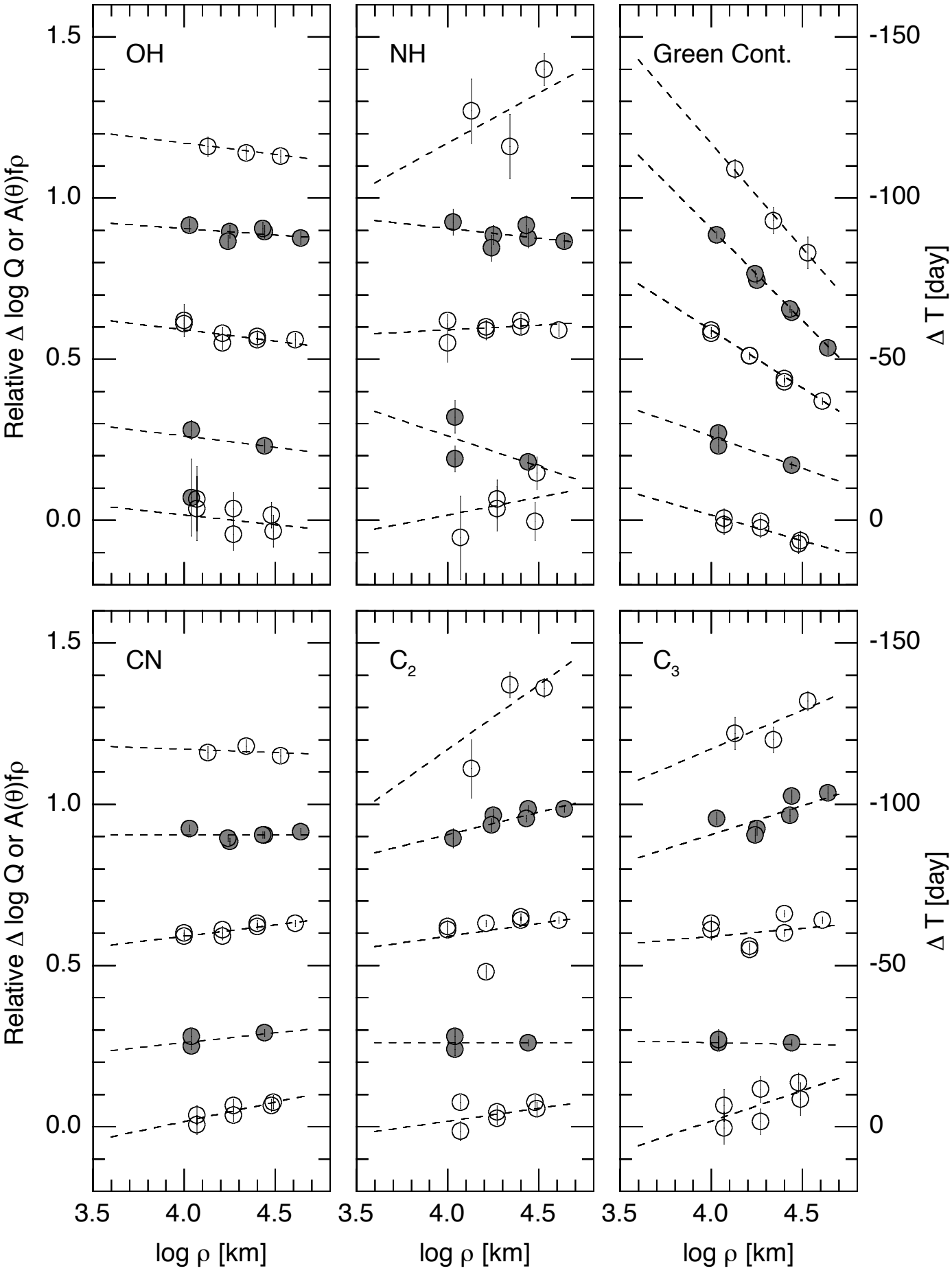
OH
NH
Green Cont.
CN
C2
C3
Relative Δ log Q or A(θ)fρ
Δ T [day]
log ρ [km]
1.5
1.0
0.5
0.0
-150
-100
-50
0
3.5
4.0
4.5

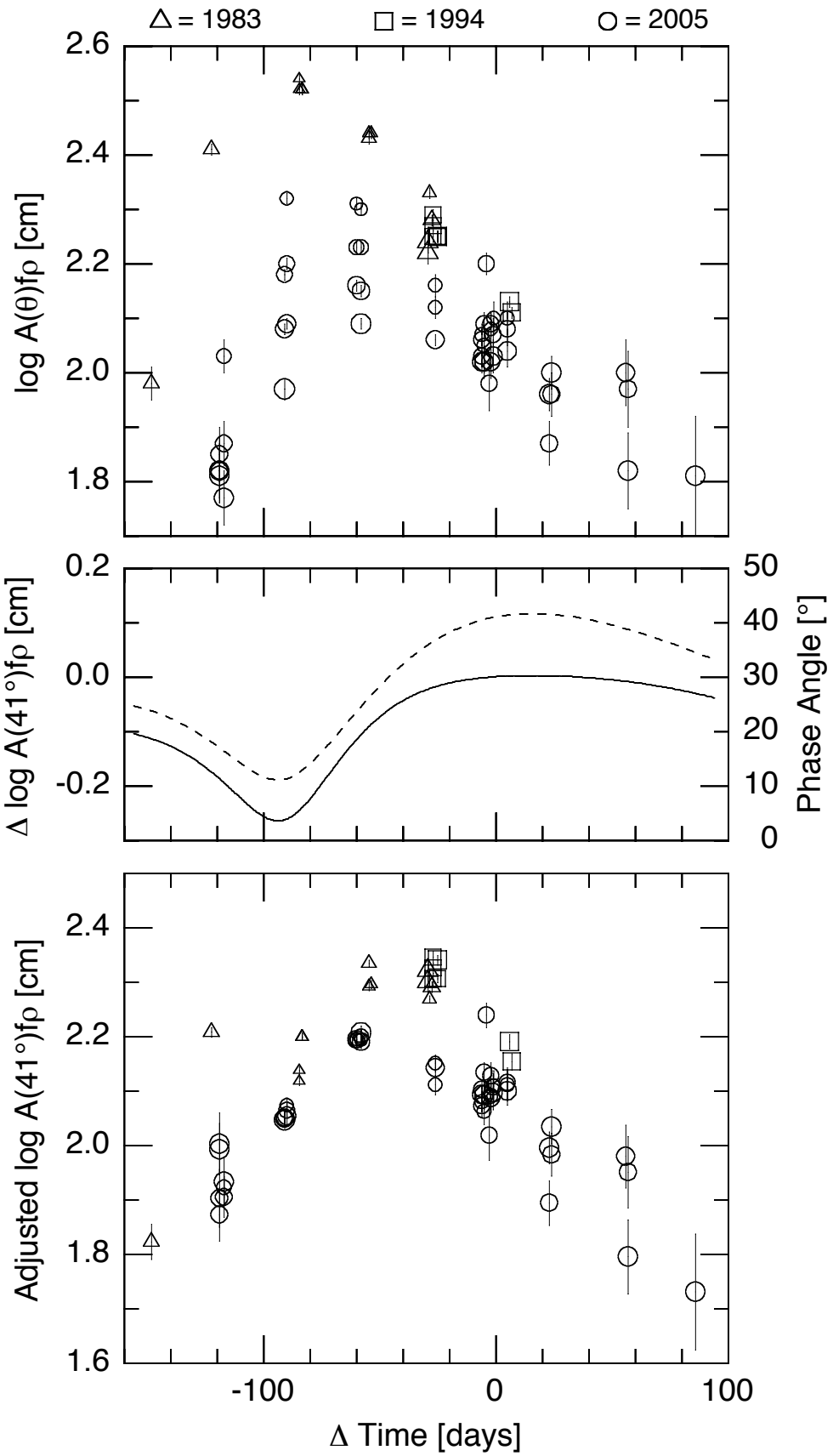
△ = 1983
□ = 1994
○ = 2005
log A(θ)fρ [cm]
2.6
2.4
2.2
2.0
1.8
Δ log A(41°)fρ [cm]
0.2
0.0
-0.2
Phase Angle [°]
50
40
30
20
10
0
Adjusted log A(41°)fρ [cm]
2.4
2.2
2.0
1.8
1.6
-100
0
100
Δ Time [days]

Figure 4

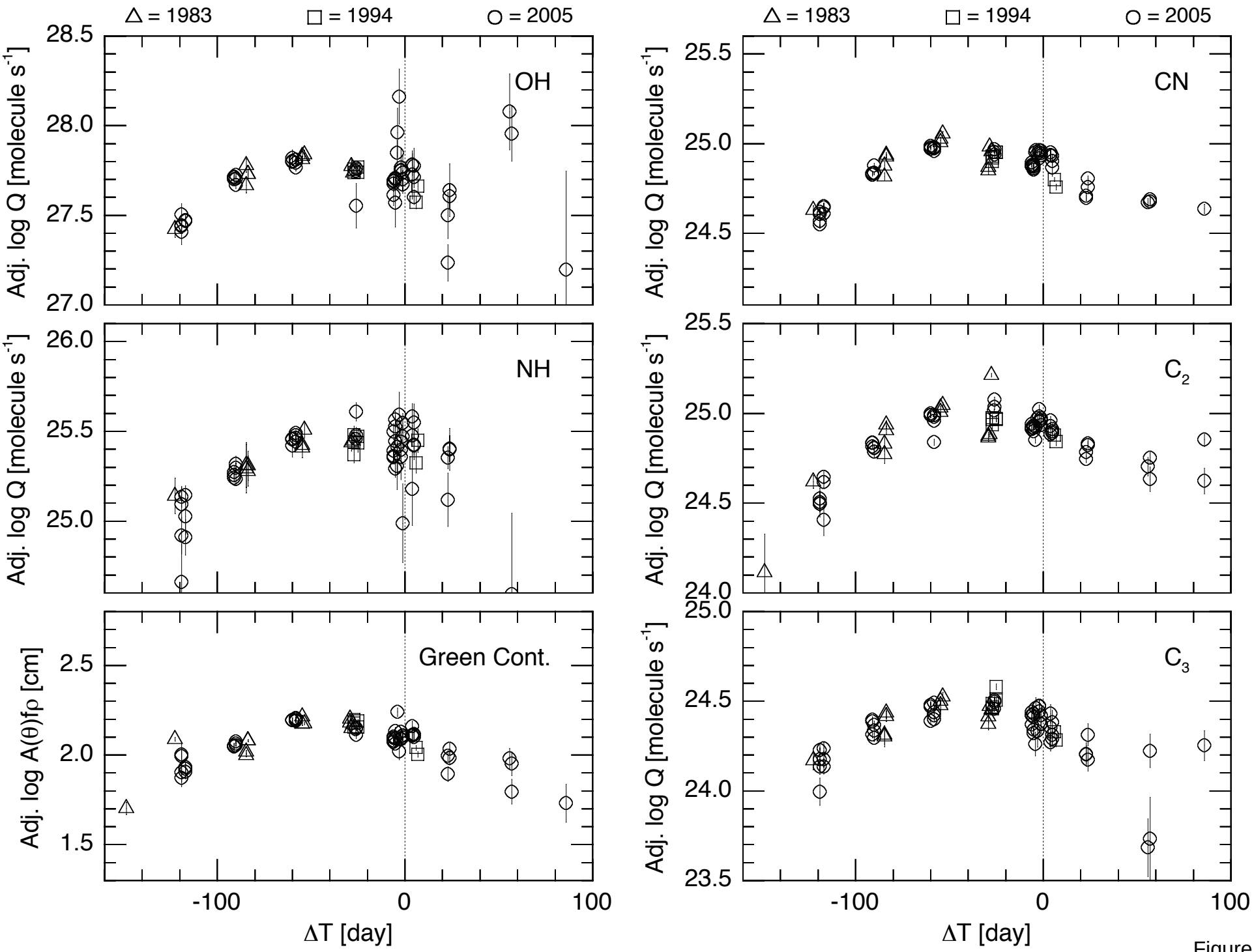
△ = 1983
□ = 1994
○ = 2005
OH
NH
Green Cont.
CN
C2
C3
Adj. log Q [molecule s-1]
Adj. log A(θ)fρ [cm]
ΔT [day]
-100
0
100

Figure 5

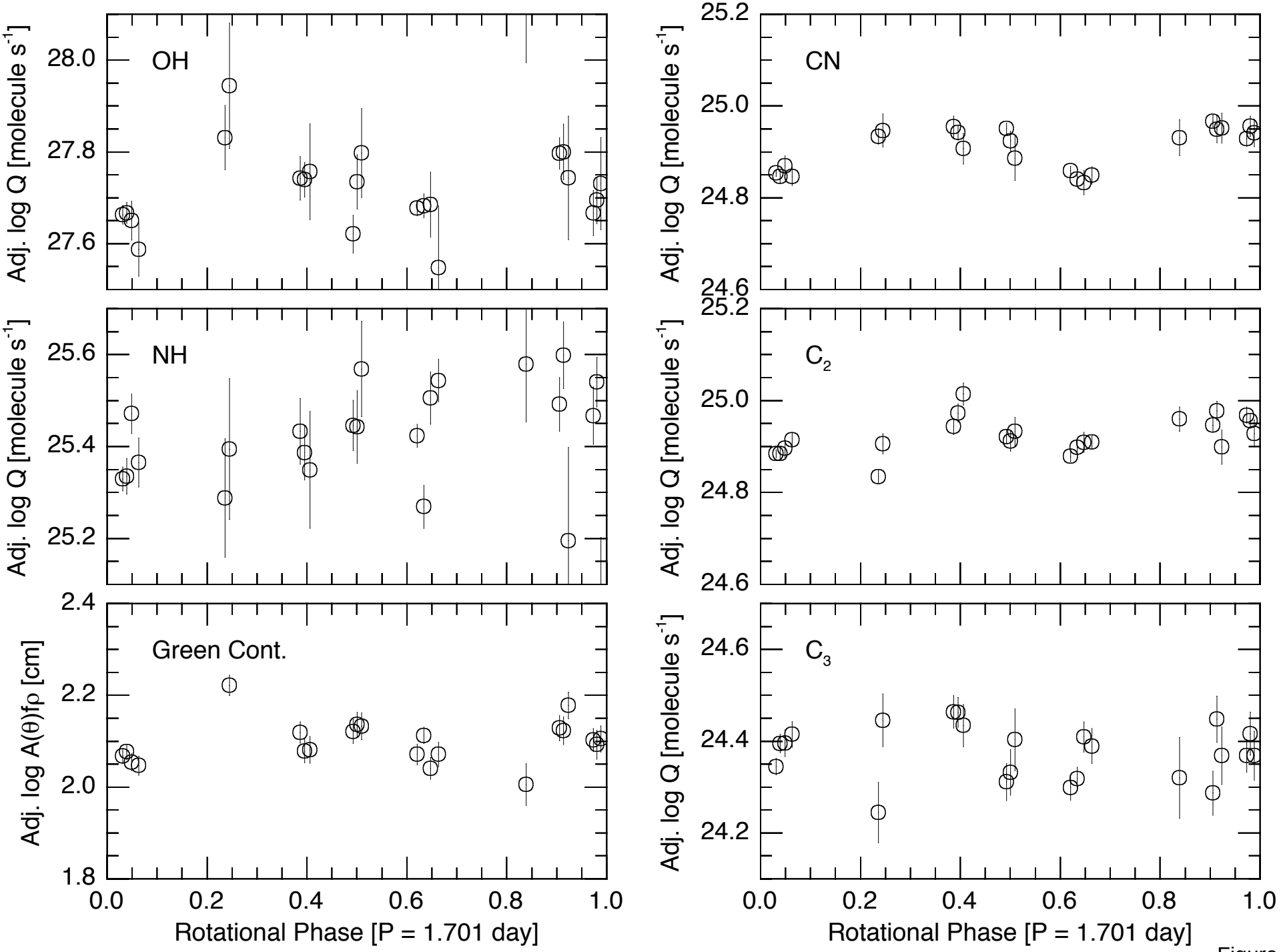
OH
NH
Green Cont.
CN
C2
C3
Adj. log Q [molecule s-1]
Adj. log A(θ)fρ [cm]
Rotational Phase [P = 1.701 day]
28.0
27.8
27.6
25.6
25.4
25.2
2.4
2.2
2.0
1.8
25.2
25.0
24.8
24.6
24.6
24.4
24.2
0.0
0.2
0.4
0.6
0.8
1.0

Figure 6

TABLE 1

Observing Circumstances and Fluorescence Efficiencies for Comet 9P/Tempel 1

UT Date	ΔT (day)	r_H (AU)	Δ (AU)	Phase Angle (°)	$\dot{r}_H$ (km s^{-1})	log L/N[a] (erg s^{-1} molecule^{-1}) OH	NH	CN	Teles[b]
1983 Feb 11.43	−148.37	2.054	1.285	22.0	−10.1	−14.558	−13.166	−12.493	L72
1983 Mar 9.41	−122.39	1.906	0.981	15.2	−9.6	−14.601	−13.154	−12.473	L72
1983 Apr 16.24	−84.56	1.711	0.759	16.0	−8.0	−14.728	−13.125	−12.431	L72
1983 Apr 17.28	−83.52	1.706	0.757	16.5	−8.0	−14.728	−13.125	−12.431	L72
1983 May 16.22	−54.58	1.589	0.757	30.4	−5.9	−14.727	−13.123	−12.431	L72
1983 May 17.19	−53.61	1.586	0.758	30.8	−5.8	−14.725	−13.124	−12.432	L72
1983 Jun 10.58	−29.22	1.520	0.825	38.6	−3.4	−14.766	−13.160	−12.478	P24
1983 Jun 11.23	−28.57	1.519	0.827	38.7	−3.3	−14.725	−13.162	−12.481	L72
1983 Jun 12.26	−27.55	1.517	0.831	38.9	−3.2	−14.726	−13.165	−12.484	L72
1994 Jun 6.20	−27.11	1.519	0.741	35.7	−3.1	−14.769	−13.167	−12.487	L31
1994 Jun 8.24	−25.06	1.516	0.747	36.3	−2.9	−14.771	−13.172	−12.494	L31
1994 Jul 9.20	+5.90	1.495	0.884	41.4	+0.7	−14.817	−13.288	−12.575	L42
1994 Jul 10.20	+6.90	1.496	0.890	41.4	+0.8	−14.814	−13.291	−12.570	L42
2005 Mar 8.29	−119.03	1.894	0.988	17.0	−9.3	−14.671	−13.147	−12.465	L42
2005 Mar 10.31	−117.01	1.883	0.968	16.4	−9.3	−14.671	−13.147	−12.464	L42
2005 Apr 5.28	−91.04	1.751	0.777	11.2	−8.2	−14.759	−13.127	−12.435	L42
2005 Apr 6.32	−90.01	1.746	0.772	11.3	−8.2	−14.759	−13.127	−12.435	L42
2005 May 6.36	−59.96	1.620	0.712	23.6	−6.2	−14.773	−13.121	−12.428	L42
2005 May 8.27	−58.05	1.613	0.713	24.5	−6.0	−14.770	−13.122	−12.430	L42
2005 Jun 9.27	−26.05	1.529	0.784	36.7	−3.0	−14.770	−13.169	−12.490	L42
2005 Jun 29.22	−6.10	1.507	0.869	40.4	−0.7	−14.819	−13.242	−12.587	L42
2005 Jun 30.23	−5.09	1.507	0.874	40.6	−0.6	−14.821	−13.246	−12.589	L42
2005 Jul 1.25	−4.07	1.507	0.879	40.7	−0.5	−14.823	−13.250	−12.590	L31
2005 Jul 2.27	−3.05	1.506	0.884	40.8	−0.4	−14.824	−13.253	−12.591	L31
2005 Jul 3.22	−2.10	1.506	0.889	40.9	−0.2	−14.826	−13.260	−12.592	L31
2005 Jul 4.23	−1.09	1.506	0.894	40.9	−0.1	−14.827	−13.263	−12.592	L31
2005 Jul 5.23	−0.09	1.506	0.899	41.0	−0.0	−14.827	−13.267	−12.592	L31
2005 Jul 6.22	+0.90	1.506	0.905	41.1	+0.1	−14.827	−13.270	−12.591	L31
2005 Jul 7.20	+1.88	1.506	0.910	41.2	+0.2	−14.826	−13.273	−12.589	L31
2005 Jul 8.20	+2.88	1.506	0.915	41.2	+0.3	−14.825	−13.276	−12.587	L31
2005 Jul 9.20	+3.88	1.507	0.921	41.3	+0.5	−14.821	−13.282	−12.582	L31
2005 Jul 10.20	+4.88	1.507	0.926	41.4	+0.6	−14.819	−13.285	−12.578	L31
2005 Jul 28.19	+22.87	1.524	1.039	41.5	+2.6	−14.714	−13.314	−12.459	L42
2005 Jul 29.19	+23.87	1.525	1.046	41.5	+2.7	−14.708	−13.314	−12.452	L42
2005 Aug 30.16	+55.84	1.606	1.311	38.9	+5.9	−14.573	−13.255	−12.339	L42
2005 Aug 31.16	+56.84	1.609	1.321	38.8	+5.9	−14.573	−13.255	−12.339	L42
2005 Sep 29.11	+85.79	1.727	1.634	34.5	+8.0	−14.565	−13.226	−12.336	L42

[a] Fluorescence efficiencies are for r_H = 1 AU, and are scaled by r_H^{-2} in the reductions.

[b] Telescope ID: L72 = Lowell 72–inch (1.8–m); L42 = Lowell 42–inch (1.1–m); L31 = 31–inch (0.8–m); P24 = Perth Observatory 24–inch (0.6–m).

TABLE 2

Photometric Fluxes and Column Abundances for Comet 9P/Tempel 1

UT Date		Aperture Size (arcsec)	Aperture log ρ (km)	log Emission Band Flux (erg cm^{-2} s^{-1}) OH	NH	CN	C_3	C_2	log Continuum Flux (erg cm^{-2} s^{-1} Å^{-1}) UV	Blue	Green	log M(ρ) (molecule) OH	NH	CN	C_3	C_2
1983 Feb	11.43	20.2	3.97	—	—	—	—	−13.13	—	—	−14.58	—	—	—	—	27.51
1983 Mar	9.41	28.5	4.01	−11.49	−12.64	−12.04	−11.78	−12.21	−14.40	—	−13.81	31.10	28.50	28.43	28.21	28.13
1983 Apr	16.21	14.1	3.59	−11.67	−12.80	−12.16	−11.94	−12.44	−14.16	—	−13.80	30.73	28.00	27.95	27.74	27.59
1983 Apr	16.27	14.1	3.59	−11.57	−12.82	−12.10	−11.94	−12.37	−14.14	—	−13.79	30.84	27.98	28.01	27.73	27.65
1983 Apr	17.27	20.2	3.74	−11.35	−12.52	−11.75	−11.55	−11.98	−14.00	—	−13.65	31.05	28.28	28.35	28.12	28.04
1983 Apr	17.30	20.2	3.74	−11.34	−12.55	−11.77	−11.57	−12.01	−13.98	—	−13.64	31.06	28.25	28.33	28.10	28.00
1983 May	16.19	28.5	3.89	−10.91	−12.02	−11.30	−11.17	−11.51	−13.87	—	−13.52	31.42	28.71	28.74	28.44	28.45
1983 May	16.25	20.2	3.74	−11.13	−12.30	−11.58	−11.43	−11.81	−14.00	—	−13.66	31.20	28.43	28.46	28.18	28.15
1983 May	17.19	20.2	3.74	−11.12	−12.21	−11.53	−11.37	−11.76	−14.01	—	−13.66	31.21	28.53	28.51	28.24	28.19
1983 Jun	10.56	77.8	4.37	—	—	−10.77	−10.74	−10.88	−13.65	—	−13.28	—	—	29.35	28.91	29.11
1983 Jun	10.60	77.8	4.37	—	—	−10.75	−10.70	−10.90	−13.66	—	−13.26	—	—	29.37	28.95	29.10
1983 Jun	11.23	20.2	3.78	−11.14	−12.25	−11.60	−11.39	−11.87	−14.15	—	−13.77	31.24	28.56	28.53	28.25	28.13
1983 Jun	12.26	40.1	4.08	−10.70	−11.72	−11.12	−10.99	−11.02	−13.82	—	−13.52	31.68	29.09	29.01	28.66	28.98
1994 Jun	6.18	81.4	4.34	−10.48	−11.25	−10.79	−10.65	−10.93	−13.48	—	−13.14	31.85	29.47	29.25	28.90	28.97
1994 Jun	6.20	81.4	4.34	−10.49	−11.35	−10.76	−10.64	−10.89	−13.59	—	−13.16	31.83	29.37	29.27	28.92	29.01
1994 Jun	6.21	81.4	4.34	−10.48	−11.29	−10.77	−10.66	−10.90	−13.56	—	−13.18	31.84	29.43	29.27	28.89	29.00
1994 Jun	8.20	81.4	4.34	−10.46	−11.26	−10.75	−10.62	−10.90	−13.69	—	−13.18	31.86	29.47	29.30	28.94	29.01
1994 Jun	8.28	114.7	4.49	−10.28	−11.05	−10.53	−10.39	−10.66	−13.69	—	−13.03	32.05	29.68	29.52	29.16	29.24
1994 Jul	9.20	104.1	4.52	−10.58	−11.35	−10.84	−10.75	−10.84	−13.62	—	−13.26	31.93	29.63	29.43	28.94	29.20
1994 Jul	10.20	73.7	4.38	−10.71	−11.48	−11.10	−10.95	−11.10	−13.87	—	−13.43	31.80	29.51	29.17	28.75	28.94
2005 Mar	8.23	97.2	4.54	−11.01	−12.06	−11.46	−11.26	−11.61	−14.39	−13.95	−13.87	31.65	29.08	29.00	28.73	28.73
2005 Mar	8.24	62.4	4.35	−11.40	−12.82	−11.75	−11.66	−11.94	−14.25	−13.94	−14.03	31.27	28.32	28.71	28.33	28.40
2005 Mar	8.34	62.4	4.35	−11.37	−12.56	−11.82	−11.52	−11.91	−14.30	−14.07	−14.06	31.29	28.58	28.64	28.47	28.43
2005 Mar	8.35	97.2	4.54	−11.07	−12.03	−11.50	−11.21	−11.62	−14.65	−13.99	−13.88	31.60	29.11	28.96	28.78	28.72
2005 Mar	10.29	97.2	4.53	−11.03	−12.00	−11.44	−11.19	−11.49	−14.18	−13.98	−13.91	31.61	29.11	28.99	28.78	28.83
2005 Mar	10.30	62.4	4.34	−11.32	−12.56	−11.71	−11.52	−11.78	−14.44	−14.04	−14.00	31.32	28.56	28.73	28.45	28.54
2005 Mar	10.33	38.5	4.13	−11.66	−12.81	−12.06	−11.75	−12.38	−14.55	−14.09	−14.04	30.98	28.31	28.37	28.22	27.94
2005 Apr	5.26	155.9	4.64	−10.43	−11.42	−10.74	−10.69	−10.84	−13.79	−13.36	−13.34	32.04	29.42	29.41	29.02	29.22
2005 Apr	5.28	97.2	4.44	−10.73	−11.74	−11.05	−10.89	−11.14	−13.99	−13.45	−13.44	31.75	29.11	29.10	28.83	28.92
2005 Apr	5.30	62.4	4.25	−11.04	−12.05	−11.36	−11.19	−11.46	−13.95	−13.53	−13.53	31.44	28.79	28.79	28.53	28.61
2005 Apr	6.30	97.2	4.43	−10.72	−11.70	−11.05	−10.93	−11.16	−13.82	−13.44	−13.42	31.75	29.14	29.09	28.78	28.89
2005 Apr	6.32	62.4	4.24	−11.06	−12.08	−11.35	−11.20	−11.48	−13.88	−13.54	−13.51	31.41	28.75	28.79	28.51	28.57
2005 Apr	6.33	38.5	4.03	−11.36	−12.36	−11.66	−11.42	−11.87	−14.08	−13.63	−13.59	31.10	28.47	28.49	28.29	28.19
2005 May	6.34	97.2	4.40	−10.53	−11.40	−10.77	−10.70	−10.86	−13.71	−13.27	−13.26	31.82	29.29	29.23	28.87	29.06
2005 May	6.35	62.4	4.21	−10.83	−11.74	−11.08	−11.01	−11.18	−13.83	−13.37	−13.37	31.52	28.95	28.92	28.57	28.74
2005 May	6.39	38.5	4.00	−11.13	−12.14	−11.44	−11.20	−11.53	−13.94	−13.51	−13.51	31.21	28.55	28.56	28.37	28.39
2005 May	8.25	155.9	4.61	−10.22	−11.08	−10.47	−10.54	−10.58	−13.58	−13.14	−13.11	32.12	29.61	29.53	29.03	29.34
2005 May	8.26	97.2	4.40	−10.53	−11.39	−10.79	−10.75	−10.87	−13.68	−13.25	−13.25	31.81	29.31	29.22	28.82	29.05
2005 May	8.27	62.4	4.21	−10.85	−11.73	−11.10	−11.00	−11.33	−13.75	−13.37	−13.37	31.49	28.97	28.90	28.57	28.59
2005 May	8.29	38.5	4.00	−11.14	−12.06	−11.43	−11.18	−11.54	−13.91	−13.54	−13.51	31.20	28.64	28.57	28.39	28.38
2005 Jun	9.24	97.2	4.44	−10.53	−11.39	−10.82	−10.71	−10.79	−13.61	−13.33	−13.34	31.85	29.39	29.28	28.89	29.17
2005 Jun	9.26	38.5	4.04	−11.12	−12.05	−11.46	−11.14	−11.43	−14.14	−13.64	−13.64	31.26	28.72	28.63	28.46	28.52
2005 Jun	9.30	38.5	4.04	−11.33	−11.92	−11.44	−11.14	−11.39	−14.25	−13.66	−13.69	31.05	28.86	28.65	28.47	28.56
2005 Jun	29.20	97.2	4.49	−10.64	−11.56	−10.99	−10.83	−10.89	−13.76	−13.41	−13.41	31.87	29.37	29.28	28.85	29.14
2005 Jun	29.21	62.4	4.29	−10.91	−11.88	−11.29	−10.98	−11.20	−14.12	−13.60	−13.57	31.59	29.05	28.98	28.70	28.83
2005 Jun	29.23	38.5	4.08	−11.26	−12.10	−11.61	−11.23	−11.53	−14.51	−13.78	−13.77	31.24	28.83	28.66	28.45	28.50
2005 Jun	29.25	62.4	4.29	−11.00	−11.84	−11.29	−10.97	−11.17	−14.09	−13.58	−13.59	31.50	29.09	28.98	28.72	28.86
2005 Jun	30.20	97.2	4.49	−10.64	−11.47	−11.00	−10.89	−10.91	−13.84	−13.41	−13.42	31.87	29.46	29.28	28.80	29.13
2005 Jun	30.22	62.4	4.30	−10.91	−11.94	−11.31	−11.07	−11.19	−13.93	−13.56	−13.54	31.60	28.99	28.97	28.62	28.84
2005 Jun	30.25	38.5	4.09	−11.23	−12.07	−11.65	−11.23	−11.52	−14.28	−13.76	−13.79	31.28	28.87	28.63	28.46	28.51

2005 Jun	30.27	97.2	4.49	−10.76	−11.36	−11.01	−10.80	−10.87	−13.71	−13.43	−13.42	31.75	29.58	29.27	28.89	29.16
2005 Jul	1.25	94.4	4.48	−10.51	−11.64	−10.94	−10.97	−10.97	−13.95	—	—	32.01	29.31	29.34	28.73	29.07
2005 Jul	1.26	58.0	4.27	−10.71	−11.89	−11.26	−10.98	−11.24	−13.83	−13.57	−13.47	31.81	29.05	29.03	28.71	28.80
2005 Jul	2.27	58.0	4.27	−10.50	−11.71	−11.27	−11.11	−11.18	−13.90	−13.59	−13.69	32.02	29.25	29.02	28.58	28.86
2005 Jul	3.20	58.0	4.27	−10.91	−11.86	−11.26	−10.97	−11.20	−14.10	−13.57	−13.58	31.62	29.10	29.04	28.73	28.85
2005 Jul	3.22	94.4	4.48	−10.61	−11.56	−10.95	−10.76	−10.85	−13.77	−13.40	−13.43	31.92	29.40	29.34	28.95	29.20
2005 Jul	3.24	36.2	4.07	−11.22	−12.30	−11.63	−11.25	−11.49	−14.17	−13.83	−13.80	31.31	28.66	28.66	28.45	28.56
2005 Jul	4.20	58.0	4.27	−11.00	−11.84	−11.28	−11.07	−11.19	−13.87	−13.67	−13.60	31.54	29.13	29.02	28.64	28.86
2005 Jul	4.22	94.4	4.49	−10.66	−11.42	−10.94	−10.81	−10.87	−13.94	−13.41	−13.43	31.87	29.55	29.36	28.90	29.18
2005 Jul	4.23	36.2	4.07	−11.25	−12.68	−11.61	−11.33	−11.57	−14.20	−13.78	−13.78	31.28	28.29	28.69	28.38	28.48
2005 Jul	4.27	36.2	4.07	−10.48	—	−11.61	−11.37	−11.53	−13.84	−13.63	−13.58	32.05	—	28.69	28.33	28.52
2005 Jul	5.21	36.2	4.07	−11.09	−12.17	−11.51	−11.22	−11.41	−14.01	−13.67	−13.68	31.45	28.81	28.79	28.49	28.64
2005 Jul	5.23	94.4	4.49	−10.80	−11.46	−10.80	−10.69	−10.77	−13.75	−13.31	−13.35	31.73	29.52	29.50	29.03	29.29
2005 Jul	5.25	36.2	4.07	−10.84	−12.03	−11.51	−11.40	−11.48	−13.89	−13.79	−13.80	31.70	28.94	28.80	28.31	28.58
2005 Jul	6.19	58.0	4.28	−10.86	−11.66	−11.13	−10.93	−11.10	−13.94	−13.50	−13.52	31.68	29.32	29.18	28.79	28.97
2005 Jul	6.23	36.2	4.07	−11.14	−11.99	−11.46	−11.16	−11.43	−14.06	−13.70	−13.74	31.41	29.00	28.85	28.56	28.63
2005 Jul	6.24	94.4	4.49	−10.55	−11.44	−10.84	−10.63	−10.77	−13.96	−13.37	−13.31	31.99	29.55	29.47	29.09	29.29
2005 Jul	6.26	36.2	4.07	—	−11.98	−11.47	−11.17	−11.44	−14.18	−13.73	−13.71	—	29.01	28.84	28.54	28.62
2005 Jul	7.19	58.0	4.28	−10.91	−11.80	−11.25	−11.00	−11.17	−13.91	−13.54	−13.59	31.64	29.19	29.06	28.73	28.90
2005 Jul	7.21	36.2	4.08	−11.16	−12.04	−11.55	−11.37	−11.52	−14.15	−13.76	−13.70	31.39	28.96	28.76	28.35	28.55
2005 Jul	8.19	58.0	4.28	−10.89	−11.74	−11.20	−11.07	−11.14	−13.82	−13.50	−13.61	31.66	29.26	29.12	28.66	28.93
2005 Jul	8.21	94.4	4.50	−10.55	−11.38	−10.87	−10.87	−10.87	−13.81	−13.39	−13.42	32.01	29.62	29.44	28.85	29.20
2005 Jul	8.22	36.2	4.08	−11.12	−12.14	−11.56	−11.28	−11.48	−14.25	−13.79	−13.79	31.43	28.87	28.76	28.45	28.59
2005 Jul	9.19	94.4	4.50	−10.59	−11.52	−10.95	−10.97	−10.91	−13.61	−13.47	−13.42	31.97	29.50	29.37	28.76	29.17
2005 Jul	9.20	58.0	4.29	−10.89	−11.75	−11.29	−11.03	−11.21	−14.09	−13.55	−13.62	31.66	29.26	29.03	28.71	28.87
2005 Jul	9.22	36.2	4.08	−11.27	−12.51	−11.61	−11.35	−11.63	−14.05	−13.75	−13.74	31.29	28.51	28.70	28.38	28.46
2005 Jul	10.19	94.4	4.50	−10.76	−11.57	−10.97	−10.96	−10.94	−13.57	−13.49	−13.43	31.80	29.46	29.35	28.78	29.15
2005 Jul	10.20	58.0	4.29	−10.95	−11.91	−11.31	−11.15	−11.28	−13.99	−13.57	−13.60	31.60	29.11	29.01	28.58	28.80
2005 Jul	10.22	36.2	4.08	−11.21	−12.14	−11.68	−11.33	−11.60	−14.46	−13.77	−13.80	31.34	28.88	28.63	28.41	28.48
2005 Jul	28.19	97.2	4.56	−11.05	−11.68	−11.10	−11.10	−11.11	—	−13.60	−13.56	31.51	29.48	29.20	28.75	29.08
2005 Jul	28.20	62.4	4.37	−11.06	−12.22	−11.38	−11.28	−11.37	−14.21	−13.83	−13.85	31.50	28.94	28.93	28.57	28.82
2005 Jul	29.19	97.2	4.57	−10.68	−11.63	−10.99	−11.13	−11.04	−13.85	−13.66	−13.53	31.88	29.54	29.32	28.73	29.16
2005 Jul	29.20	62.4	4.37	−10.92	−11.95	−11.32	−11.17	−11.32	−14.09	−13.81	−13.76	31.64	29.22	28.99	28.68	28.88
2005 Aug	30.16	62.4	4.47	−10.46	—	−11.41	−11.94	−11.56	—	−13.90	−13.86	32.21	—	29.03	28.15	28.88
2005 Aug	31.15	77.8	4.57	−10.46	−12.65	−11.27	−11.81	−11.37	−13.90	−13.82	−13.95	32.22	28.71	29.18	28.29	29.08
2005 Aug	31.17	48.6	4.37	—	—	−11.56	−11.52	−11.80	—	−14.11	−14.00	—	—	28.89	28.58	28.65
2005 Sep	29.11	62.4	4.57	−11.49	—	−11.58	−11.53	−11.77	—	−14.16	−14.21	31.42	—	29.11	28.82	28.93
2005 Sep	29.12	62.4	4.57	—	—	−12.94	—	−11.55	—	−14.16	−15.87	—	—	27.75	—	29.15

TABLE 3

Photometric Production Rates for Comet 9P/Tempel 1

UT Date		ΔT (day)	log r_H (AU)	log ρ (km)	log Q^a (molecule s^{-1}) OH		NH		CN		C_3		C_2		log $A(\theta)f\rho^a$ (cm) UV		Blue		Green		log Q H_2O
1983 Feb	11.43	−148.37	0.313	3.97	—		—		—		—		24.31	.14	—		—		1.98	.03	—
1983 Mar	9.41	−122.39	0.280	4.01	27.80	.04	25.46	.08	24.92	.02	24.35	.05	24.82	.03	2.01	.05	—		2.41	.01	27.79
1983 Apr	16.21	−84.59	0.233	3.59	28.08	.04	25.62	.10	25.08	.02	24.45	.05	24.93	.04	2.36	.03	—		2.52	.01	28.10
1983 Apr	16.27	−84.54	0.233	3.59	28.19	.03	25.60	.10	25.14	.02	24.44	.05	24.99	.04	2.38	.03	—		2.54	.01	28.20
1983 Apr	17.27	−83.54	0.232	3.74	28.13	.03	25.62	.07	25.21	.01	24.59	.03	25.11	.02	2.36	.02	—		2.52	.01	28.14
1983 Apr	17.30	−83.50	0.232	3.74	28.13	.03	25.59	.07	25.20	.01	24.57	.03	25.08	.02	2.38	.02	—		2.52	.01	28.15
1983 May	16.19	−54.61	0.201	3.89	28.20	.02	25.74	.03	25.31	.01	24.67	.02	25.22	.01	2.27	.02	—		2.43	.01	28.23
1983 May	16.25	−54.55	0.201	3.74	28.23	.03	25.72	.05	25.28	.01	24.63	.02	25.18	.01	2.30	.02	—		2.44	.01	28.27
1983 May	17.19	−53.61	0.200	3.74	28.24	.02	25.82	.04	25.33	.01	24.68	.02	25.22	.01	2.28	.02	—		2.44	.01	28.27
1983 Jun	10.56	−29.24	0.182	4.37	—		—		25.16	.02	24.59	.03	25.11	.02	2.08	.03	—		2.22	.02	—
1983 Jun	10.60	−29.20	0.182	4.37	—		—		25.18	.02	24.63	.03	25.10	.02	2.08	.03	—		2.24	.02	—
1983 Jun	11.23	−28.57	0.182	3.78	28.17	.04	25.75	.04	25.26	.01	24.63	.02	25.06	.01	2.14	.03	—		2.33	.01	28.22
1983 Jun	12.26	−27.55	0.181	4.08	28.11	.02	25.77	.02	25.25	.01	24.64	.01	25.42	.01	2.17	.02	—		2.28	.01	28.15
1994 Jun	6.18	−27.12	0.182	4.34	27.86	.02	25.72	.05	25.09	.01	24.60	.02	25.01	.02	2.19	.04	—		2.29	.01	27.90
1994 Jun	6.20	−27.11	0.182	4.34	27.84	.02	25.61	.05	25.12	.01	24.62	.02	25.05	.02	2.08	.04	—		2.27	.01	27.89
1994 Jun	6.21	−27.09	0.182	4.34	27.86	.02	25.68	.04	25.11	.01	24.59	.02	25.04	.02	2.11	.04	—		2.25	.01	27.90
1994 Jun	8.20	−25.10	0.181	4.34	27.87	.02	25.71	.03	25.14	.01	24.64	.01	25.04	.01	1.98	.03	—		2.25	.01	27.92
1994 Jun	8.28	−25.02	0.181	4.49	27.83	.02	25.68	.05	25.15	.01	24.73	.02	25.06	.02	1.83	.06	—		2.25	.01	27.87
1994 Jul	9.20	+5.90	0.175	4.52	27.66	.04	25.57	.06	25.00	.01	24.48	.03	24.97	.01	2.00	.05	—		2.13	.01	27.70
1994 Jul	10.20	+6.90	0.175	4.38	27.76	.04	25.69	.07	24.95	.02	24.42	.04	24.92	.02	1.91	.07	—		2.11	.01	27.80
2005 Mar	8.23	−119.09	0.277	4.54	27.46	.06	25.11	.10	24.64	.03	24.23	.06	24.56	.05	1.61	.20	1.72	.07	1.82	.06	27.46
2005 Mar	8.24	−119.08	0.277	4.35	27.38	.07	24.67	.21	24.64	.03	24.03	.08	24.53	.07	1.94	.10	1.92	.05	1.85	.05	27.38
2005 Mar	8.34	−118.98	0.277	4.35	27.41	.02	24.93	.10	24.57	.02	24.17	.04	24.56	.06	1.88	.08	1.79	.05	1.82	.05	27.40
2005 Mar	8.35	−118.97	0.277	4.54	27.40	.02	25.15	.06	24.60	.03	24.28	.04	24.55	.04	1.34	.19	1.68	.06	1.81	.05	27.40
2005 Mar	10.29	−117.03	0.275	4.53	27.43	.02	25.16	.05	24.64	.02	24.29	.03	24.67	.03	1.80	.09	1.67	.06	1.77	.05	27.43
2005 Mar	10.30	−117.02	0.275	4.34	27.44	.02	24.92	.10	24.67	.02	24.17	.04	24.68	.04	1.73	.10	1.81	.04	1.87	.04	27.44
2005 Mar	10.33	−116.99	0.275	4.13	27.46	.03	25.03	.10	24.65	.02	24.19	.05	24.42	.09	1.84	.08	1.97	.03	2.03	.03	27.45
2005 Apr	5.26	−91.06	0.243	4.64	27.66	.02	25.26	.02	24.87	.01	24.45	.02	24.88	.01	1.83	.06	1.93	.02	1.97	.02	27.67
2005 Apr	5.28	−91.04	0.243	4.44	27.68	.02	25.27	.03	24.86	.01	24.44	.02	24.88	.01	1.83	.06	2.04	.02	2.08	.01	27.69
2005 Apr	5.30	−91.02	0.243	4.25	27.68	.02	25.28	.03	24.84	.01	24.34	.02	24.86	.02	2.07	.03	2.16	.01	2.18	.01	27.69
2005 Apr	6.30	−90.02	0.242	4.43	27.69	.02	25.31	.03	24.86	.01	24.38	.02	24.85	.01	1.99	.04	2.05	.02	2.09	.01	27.70
2005 Apr	6.32	−90.01	0.242	4.24	27.65	.02	25.24	.04	24.85	.01	24.32	.02	24.83	.02	2.13	.03	2.15	.01	2.20	.01	27.67
2005 Apr	6.33	−89.99	0.242	4.03	27.70	.02	25.32	.04	24.88	.01	24.37	.02	24.79	.03	2.14	.03	2.27	.01	2.32	.01	27.71
2005 May	6.34	−59.98	0.210	4.40	27.77	.02	25.47	.02	25.01	.01	24.52	.01	25.03	.01	2.00	.04	2.12	.01	2.16	.01	27.80
2005 May	6.35	−59.97	0.210	4.21	27.78	.02	25.46	.03	24.99	.01	24.41	.02	25.01	.01	2.08	.04	2.21	.01	2.23	.01	27.81
2005 May	6.39	−59.93	0.210	4.00	27.82	.05	25.42	.06	24.97	.01	24.47	.03	25.00	.02	2.18	.05	2.28	.01	2.31	.01	27.85
2005 May	8.25	−58.07	0.208	4.61	27.76	.02	25.46	.02	25.01	.01	24.50	.01	25.02	.01	1.93	.03	2.04	.01	2.09	.01	27.79
2005 May	8.26	−58.06	0.208	4.40	27.76	.02	25.49	.02	25.00	.01	24.46	.01	25.02	.01	2.03	.03	2.13	.01	2.15	.01	27.79
2005 May	8.27	−58.05	0.208	4.21	27.75	.02	25.47	.02	24.97	.01	24.42	.01	24.86	.02	2.16	.02	2.21	.01	2.23	.01	27.78
2005 May	8.29	−58.04	0.208	4.00	27.81	.02	25.49	.02	24.98	.01	24.49	.02	24.99	.02	2.21	.02	2.25	.01	2.30	.01	27.84
2005 Jun	9.24	−26.08	0.184	4.44	27.71	.02	25.47	.02	24.98	.01	24.50	.01	25.06	.01	2.10	.04	2.05	.02	2.06	.01	27.75
2005 Jun	9.26	−26.06	0.184	4.04	27.76	.03	25.48	.04	24.94	.01	24.50	.02	25.04	.02	1.97	.06	2.14	.02	2.16	.02	27.80
2005 Jun	9.30	−26.02	0.184	4.04	27.55	.12	25.61	.05	24.97	.02	24.51	.03	25.08	.02	1.87	.11	2.12	.02	2.12	.02	27.60
2005 Jun	29.20	−6.12	0.178	4.49	27.65	.02	25.37	.03	24.91	.01	24.42	.02	24.96	.01	1.98	.04	2.01	.02	2.02	.02	27.70
2005 Jun	29.21	−6.11	0.178	4.29	27.67	.02	25.37	.04	24.89	.01	24.45	.02	24.94	.01	1.82	.07	2.00	.02	2.06	.02	27.72
2005 Jun	29.23	−6.09	0.178	4.08	27.67	.04	25.50	.04	24.90	.02	24.43	.03	24.93	.02	1.63	.11	2.04	.02	2.07	.02	27.71
2005 Jun	29.25	−6.07	0.178	4.29	27.59	.06	25.40	.05	24.89	.02	24.47	.03	24.97	.01	1.84	.10	2.03	.02	2.03	.02	27.63
2005 Jun	30.20	−5.12	0.178	4.49	27.66	.02	25.46	.03	24.91	.01	24.37	.03	24.95	.01	1.91	.06	2.00	.03	2.02	.02	27.70
2005 Jun	30.22	−5.10	0.178	4.30	27.68	.03	25.30	.05	24.88	.01	24.37	.02	24.95	.01	2.01	.05	2.05	.02	2.09	.02	27.73
2005 Jun	30.25	−5.07	0.178	4.09	27.70	.07	25.53	.06	24.86	.03	24.44	.03	24.94	.02	1.87	.10	2.06	.02	2.05	.02	27.74
2005 Jun	30.27	−5.05	0.178	4.49	27.53	.13	25.58	.05	24.90	.02	24.46	.04	24.98	.01	2.03	.10	1.98	.04	2.02	.03	27.58

2005 Jul	1.25	–4.07	0.178	4.48	27.81	.07	25.32	.13	24.98	.02	24.31	.07	24.90	.02	1.81	.21	—	.11	—	.08	27.85
2005 Jul	1.26	–4.06	0.178	4.27	27.94	.14	25.42	.15	24.98	.04	24.49	.06	24.95	.02	2.14	.16	2.07	.04	2.20	.02	27.98
2005 Jul	2.27	–3.05	0.178	4.27	28.14	.15	25.60	.13	24.96	.04	24.36	.09	25.00	.03	2.07	.19	2.06	.05	1.98	.05	28.19
2005 Jul	3.20	–2.12	0.178	4.27	27.73	.05	25.45	.07	24.98	.02	24.50	.04	24.98	.02	1.87	.12	2.08	.03	2.09	.02	27.78
2005 Jul	3.22	–2.10	0.178	4.48	27.71	.04	25.41	.06	24.98	.02	24.52	.03	25.03	.02	1.99	.10	2.04	.03	2.02	.03	27.75
2005 Jul	3.24	–2.08	0.178	4.07	27.76	.10	25.36	.13	24.92	.03	24.45	.05	25.03	.02	2.01	.12	2.02	.04	2.08	.03	27.81
2005 Jul	4.20	–1.12	0.178	4.27	27.65	.05	25.48	.06	24.95	.02	24.40	.04	25.00	.02	2.11	.08	1.98	.04	2.07	.03	27.70
2005 Jul	4.22	–1.11	0.178	4.49	27.66	.05	25.56	.05	24.99	.02	24.47	.05	25.01	.02	1.83	.16	2.03	.04	2.03	.03	27.70
2005 Jul	4.23	–1.09	0.178	4.07	27.73	.10	24.99	.22	24.95	.03	24.38	.05	24.94	.03	1.98	.12	2.07	.03	2.10	.03	27.77
2005 Jul	4.27	–1.06	0.178	4.07	28.50	.10	—		24.95	.04	24.33	.08	24.98	.03	2.35	.11	2.22	.03	2.30	.02	28.54
2005 Jul	5.21	–0.12	0.178	4.07	27.90	.05	25.50	.08	25.04	.02	24.48	.03	25.10	.02	2.18	.07	2.19	.02	2.20	.02	27.94
2005 Jul	5.23	–0.09	0.178	4.49	27.52	.07	25.52	.05	25.13	.02	24.60	.03	25.11	.02	2.02	.10	2.13	.03	2.12	.02	27.56
2005 Jul	5.25	–0.07	0.178	4.07	28.14	.11	25.63	.10	25.05	.02	24.30	.06	25.03	.03	2.29	.09	2.07	.04	2.08	.03	28.19
2005 Jul	6.19	+0.87	0.178	4.28	27.79	.03	25.67	.04	25.11	.01	24.55	.03	25.09	.01	2.04	.08	2.16	.02	2.16	.02	27.84
2005 Jul	6.23	+0.91	0.178	4.07	27.85	.08	25.68	.07	25.10	.02	24.55	.04	25.08	.02	2.12	.09	2.16	.03	2.14	.03	27.89
2005 Jul	6.24	+0.92	0.178	4.49	27.77	.07	25.54	.06	25.09	.02	24.66	.04	25.11	.01	1.81	.17	2.08	.03	2.15	.02	27.82
2005 Jul	6.26	+0.94	0.178	4.07	—	.99	25.69	.11	25.09	.04	24.53	.06	25.07	.03	2.01	.17	2.13	.04	2.17	.03	—
2005 Jul	7.19	+1.87	0.178	4.28	27.74	.04	25.53	.06	24.99	.02	24.49	.03	25.03	.02	2.07	.09	2.12	.03	2.09	.02	27.79
2005 Jul	7.21	+1.89	0.178	4.08	27.82	.07	25.64	.07	25.00	.02	24.34	.05	25.00	.02	2.04	.11	2.10	.03	2.18	.02	27.87
2005 Jul	8.19	+2.87	0.178	4.28	27.76	.04	25.59	.05	25.04	.01	24.42	.04	25.05	.02	2.17	.07	2.16	.02	2.07	.03	27.80
2005 Jul	8.21	+2.89	0.178	4.50	27.78	.03	25.61	.04	25.06	.01	24.42	.04	25.01	.01	1.97	.10	2.06	.03	2.05	.02	27.83
2005 Jul	8.22	+2.90	0.178	4.08	27.86	.07	25.54	.10	25.00	.03	24.44	.05	25.03	.02	1.94	.13	2.08	.04	2.10	.03	27.91
2005 Jul	9.19	+3.87	0.178	4.50	27.74	.03	25.49	.06	24.98	.01	24.32	.05	24.98	.02	2.17	.08	1.98	.04	2.05	.03	27.78
2005 Jul	9.20	+3.88	0.178	4.29	27.76	.06	25.59	.07	24.95	.03	24.46	.05	24.99	.02	1.90	.15	2.11	.03	2.07	.03	27.80
2005 Jul	9.22	+3.90	0.178	4.08	27.72	.13	25.18	.20	24.94	.03	24.36	.06	24.89	.04	2.14	.12	2.11	.04	2.15	.03	27.76
2005 Jul	10.19	+4.87	0.178	4.50	27.56	.04	25.44	.05	24.96	.01	24.34	.04	24.95	.02	2.21	.06	1.97	.04	2.04	.03	27.61
2005 Jul	10.20	+4.88	0.178	4.29	27.69	.06	25.43	.08	24.92	.02	24.34	.05	24.92	.02	2.00	.11	2.10	.03	2.08	.03	27.74
2005 Jul	10.22	+4.90	0.178	4.08	27.77	.10	25.55	.10	24.87	.05	24.39	.07	24.92	.03	1.74	.20	2.10	.03	2.10	.03	27.81
2005 Jul	28.19	+22.87	0.183	4.56	27.19	.10	25.37	.06	24.73	.01	24.26	.05	24.80	.02	—	.11	1.90	.04	1.96	.03	27.23
2005 Jul	28.20	+22.88	0.183	4.37	27.47	.13	25.13	.15	24.73	.03	24.24	.07	24.82	.03	1.81	.17	1.87	.05	1.87	.04	27.52
2005 Jul	29.19	+23.87	0.183	4.57	27.56	.07	25.42	.07	24.84	.01	24.23	.06	24.88	.02	1.98	.12	1.85	.05	2.00	.03	27.60
2005 Jul	29.20	+23.88	0.183	4.37	27.61	.15	25.41	.12	24.78	.03	24.35	.06	24.87	.03	1.93	.17	1.89	.06	1.96	.04	27.65
2005 Aug	30.16	+55.84	0.206	4.47	28.04	.21	—		24.70	.02	23.73	.16	24.75	.05	—		1.94	.08	2.00	.06	28.08
2005 Aug	31.15	+56.83	0.207	4.57	27.91	.15	24.61	.45	24.71	.02	23.79	.23	24.81	.03	2.18	.18	1.92	.07	1.82	.07	27.94
2005 Aug	31.17	+56.85	0.207	4.37	—		—		24.71	.03	24.26	.09	24.67	.07	—		1.84	.10	1.97	.07	—
2005 Sep	29.11	+85.79	0.237	4.57	27.15	.55	—		24.67	.03	24.31	.08	24.68	.07	—		1.84	.11	1.81	.11	27.16
2005 Sep	29.12	+85.80	0.237	4.57	—		—		23.31	.61	—	.18	24.91	.04	—		1.84	.12	0.15	.57	—

[a] Production rates, followed by uncertainties.

TABLE 4

Aperture Coefficients and Secular Changes for Comet 9P/Tempel 1

Species	Mean Aperture Trend Coeff.	Secular Change Compared to 1983		
		1983	1994	2005
OH	–0.08	1.00	~0.56	0.42
NH	+0.03	1.00	~0.81	0.48
CN	+0.06	1.00	~0.76	0.51
C_3	+0.10	1.00	~0.83	0.66
C_2	+0.10	1.00	~0.72	0.63
Green Cont. [a]	*a*	1.00	~1.07	0.76

[a] For the dust continuum, the aperture trend varied with time from perihelion in days: $-0.1335 + 0.003429*\Delta T - 0.0000101666*\Delta T^2$

TABLE 5

Abundance Ratios for Comet 9P/Tempel 1

	log Production Rate Ratios (X/OH)		
Species	1983	1994	2005
OH	0.00	0.00	0.00
NH	–2.44±.07	–2.19±.05	–2.36±.22
CN	–2.90±.04	–2.79±.04	–2.84±.15
C_3	–3.53±.06	–3.30±.07	–3.36±.23
C_2	–2.99±.11	–2.87±.04	–2.83±.16
UV Cont.[a]	–26.05±.13	–25.77±.11	–25.72±.21
Blue Cont.[a]	—	—	–25.62±.29
Green Cont.[a]	–25.88±.11	–25.56±.04	–25.62±.16

[a] For the dust continuum, the ratio of $A(\theta)f\rho$ to Q(OH) has units of cm sec mol^{-1}.